Proceedings of the International Workshop
Future Directions in Difference Equations.
June 13-17, 2011, Vigo, Spain.
PAGES 15–50

Contact bifurcations related to critical sets and focal points in iterated maps of the plane

Gian-Italo Bischi*, Laura Gardini* and Christian Mira

*University of Urbino, Italy

gian.bischi@uniurb.it; laura.gardini@uniurb.it; c.mira@free.fr

Abstract

In this survey article we briefly describe some properties of difference equations obtained by the iterated applications of two-dimensional maps of the plane and we try to characterize the qualitative changes (or bifurcations) of the asymptotic behavior of the solutions, as some parameters are varied, in terms of contacts between particular curves and invariant sets which characterize the global properties of the iterated maps. In particular we consider the role of critical curves in noninvertible maps of the plane and the contacts involving focal points and prefocal sets in maps of the plane characterized by the presence (in the map or in some inverse map) of a denominator that vanishes along a curve of the plane. The effects of the global bifurcations given by contacts involving such singular curves on the attractors and their basins are described through some examples.

1 Introduction

Second order difference equations are often expressed in the form of a two-dimensional discrete dynamical system

$$\mathbf{x}_{n+1} = T(\mathbf{x}_n) \tag{1}$$

where $\mathbf{x} \in \mathbb{R}^2$, T is a map of the plane into itself and $t \in \mathbb{N}$. Given an initial condition $x_0 \subseteq \mathbb{R}^2$ in the domain of the map T the sequence $\mathbf{x}_t$ generated by the iteration of a map T is obtained inductively. So, even if a closed form (analytic) solution cannot be obtained in general, the study of the qualitative asymptotic properties of the sequences generated is an interesting and useful goal. Indeed, the sequence defined by (1) may converge to a given steady state (or equilibrium) or to a more complex attractor, that may be periodic, quasi-periodic or chaotic. In such cases, a delimitation of a bounded region of the plane where the system dynamics are ultimately trapped, despite of the complexity of the long-run time patterns, may be an useful information for practical applications. Moreover, as some parameter is varied, global bifurcations may cause sudden qualitative changes in the properties of the attracting sets (see the contact bifurcations in [40] and the so called *crises* in [31]).

Another problem which often arises in the study of nonlinear maps concerns the existence of several attracting sets, each with its own basin of attraction. This naturally leads to the delimitation of the basins of attraction and their changes as the parameters of the model vary.

These two problems lead to two different routes to complexity, one related to the complexity of the attracting sets which characterize the long run time evolution of the dynamic process, the other one related to the complexity of the boundaries which separate the basins when several coexisting attractors are present. These two different kinds of complexity are not related in general, in the sense that very complex attractors may have simple basin boundaries, whereas boundaries which separate the basins of simple attractors, such as coexisting stable equilibria, may have very complex structures.

Both the questions outlined above require an analysis of the global dynamical properties of the dynamical system, that is, an analysis which is not based on the linear approximation of the map (1). When it is *noninvertible*, the global dynamical properties can be usefully characterized by the method of critical sets, a powerful tool introduced in the seventies (see [29, 37] and [40]). Geometrically, the action of a noninvertible map can be expressed by saying that it "folds and pleats" the phase space along the critical sets, so that two or more distinct points are mapped into the same point, or, equivalently, that several inverses are defined which "unfold" the plane. The iterated application of a noninvertible map repeatedly folds the state space, and often this allows one to define a bounded region where asymptotic dynamics are trapped. Conversely, the iterated application of the inverses repeatedly unfolds the state space, so that a neighborhood of an attractor may have preimages far from it. This may give rise to complicated topological structures of the basins, that can even be formed by the union of several disjoint portions. If a parameter variation causes a crossing between a basin boundary and a critical set, so that a portion of a basin enters a region where an higher number of inverses is defined, then new components of the basin suddenly appear after the contact. The detection of these *contact bifurcations* are easily obtained in one-dimensional nonlinear maps, whereas in the study of two-dimensional maps an interplay between analytic, geometric and numerical methods is often necessary, and contacts are often shown by computer-assisted proofs. Instead, an extension to the study of higher dimensional noninvertible maps leads to nontrivial practical problems, as the visualization, in a computer screen, of contacts between objects in a space of dimension greater than two becomes a difficult task.

An important role of critical sets has been recently emphasized in problems of *chaos synchronization*, i.e. chaotic dynamical systems with an invariant submanifold of lower dimensionality than the total phase. *Milnor attractors* which are, unstable in Lyapunov sense appear quite naturally in this context, together with new phenomena like *on-off intermittency* and *riddled basins*, as well as *riddling* and *blowout* bifurcations (see [10, 21] and [33]). Even if the occurrence of these bifurcations is detected through the study of the *transverse Lyapunov exponents*, their effects strongly depend on the action of the nonlinearities far from the invariant subset. When the iterated map is noninvertible, as generally occurs in problems of chaos synchronization, the method of critical sets can be used to characterize the global fate of the locally repelled trajectories after a riddling bifurcation, as proposed in [4, 6] where the critical curves are used to obtain the boundary of a compact trapping region inside which intermittency and blowout phenomena are confined.

Another example where the critical curve may play an important role comes from the study of iterated rational maps not defined everywhere due to the vanishing of a denominator. The global bifurcations of noninvertible maps with a vanishing denominator have been recently characterized by contacts between stable or unstable manifolds, critical sets, and new kinds of singularities, called *focal points*, *prefocal curves* and *sets of nondefinition*, recently introduced in [13, 15] and [16] (see also [14] and [26]).

Some general properties of noninvertible maps of the plane and the contact bifurcations involving the critical curves are described in Section 2, their applications to the study of chaotic

synchronization, riddling and on-off intermittency phenomena is summarized in Section 3 and some definitions and properties of iterated maps with a vanishing denominator are given in Section 4.

2 Noninvertible maps and critical sets

In this section we give some definitions, properties and simple examples about recurrences represented by the iteration of noninvertible maps.

2.1 Definitions and simple examples

A map $T : S \to S$, $S \subseteq \mathbb{R}^2$, defined by $\mathbf{x}' = T(\mathbf{x})$, transforms a point $\mathbf{x} \in S$ into a unique point $\mathbf{x}' \in S$. The point $\mathbf{x}'$ is called the *rank*-1 *image* of $\mathbf{x}$, and a point $\mathbf{x}$ such that $T(\mathbf{x}) = \mathbf{x}'$ is a *rank*-1 *preimage* of $\mathbf{x}'$. If $\mathbf{x} \neq \mathbf{y}$ implies $T(\mathbf{x}) \neq T(\mathbf{y})$ for each $\mathbf{x}$, $\mathbf{y}$ in S, then T is an *invertible map* in S, because the inverse mapping $\mathbf{x} = T^{-1}(\mathbf{x}')$ is uniquely defined; otherwise T is a said to be a *noninvertible map*, because points $\mathbf{x}$ exist that have several rank-1 preimages, i.e. the inverse relation $\mathbf{x} = T^{-1}(\mathbf{x}')$ is multivalued. So, noninvertible means "many-to-one", that is, distinct points $\mathbf{x} \neq \mathbf{y}$ may have the same image, $T(\mathbf{x}) = T(\mathbf{y}) = \mathbf{x}'$.

Geometrically, the action of a noninvertible map can be expressed by saying that it "folds and pleats" the space S, so that distinct points are mapped into the same point. This is equivalently stated by saying that several inverses are defined in some points of S, and these inverses "unfold" S.

For a noninvertible map, S can be subdivided into regions Z_k, $k \geq 0$, whose points have k distinct rank-1 preimages. Generally, for a continuous map, as the point $\mathbf{x}'$ varies in $\mathbb{R}^n$, pairs of preimages appear or disappear as it crosses the boundaries separating different regions. Hence, such boundaries are characterized by the presence of at least two coincident (merging) preimages. This leads us to the definition of the *critical sets*, one of the distinguishing features of noninvertible maps (see [29] and [40]):

Definition 2.1. *The* critical set CS *of a continuous map T is defined as the locus of points having at least two coincident rank-*1 *preimages, located on a set CS_{-1}, called* set of merging preimages.

Portions of CS separate regions Z_k of the plane characterized by a different number of rank-1 preimages, for example Z_k and Z_{k+2} (this is the standard occurrence for continuous maps). In the case of a two-dimensional noninvertible map the critical set CS coincides with the notion of *critical curve* LC[1], and can be seen as the 2-dimensional generalization of the notion of local minimum or local maximum value of a one-dimensional map. The set CS_{-1} is the *fold curve* LC_{-1} of a two-dimensional noninvertible maps, the generalization of local extremum point of a one-dimensional map.

As an illustration, we consider the one-dimensional quadratic map (logistic map)

$$x' = f(x) = \mu x(1 - x). \tag{2}$$

This map has a unique critical point $c = \mu/4$, which separates the real line into the two subsets: $Z_0 = (c, +\infty)$, where no inverses are defined, and $Z_2 = (-\infty, c)$, whose points have two rank-1

[1]This terminology, and notation, originates from the notion of critical point as it is used in the classical works of Julia and Fatou.

preimages. These preimages can be computed by the two inverses

$$x_1 = f_1^{-1}(x') = \frac{1}{2} - \frac{\sqrt{\mu\,(\mu - 4x')}}{2\mu}; \quad x_2 = f_2^{-1}(x') = \frac{1}{2} + \frac{\sqrt{\mu\,(\mu - 4x')}}{2\mu}. \tag{3}$$

If $x' \in Z_2$, its two rank-1 preimages, computed according to (3), are located symmetrically with respect to the point $c_{-1} = 1/2 = f_1^{-1}(\mu/4) = f_2^{-1}(\mu/4)$. Hence, c_{-1} is the point where the two merging preimages of c are located. As the map (2) is differentiable, at c_{-1} the first derivative vanishes.

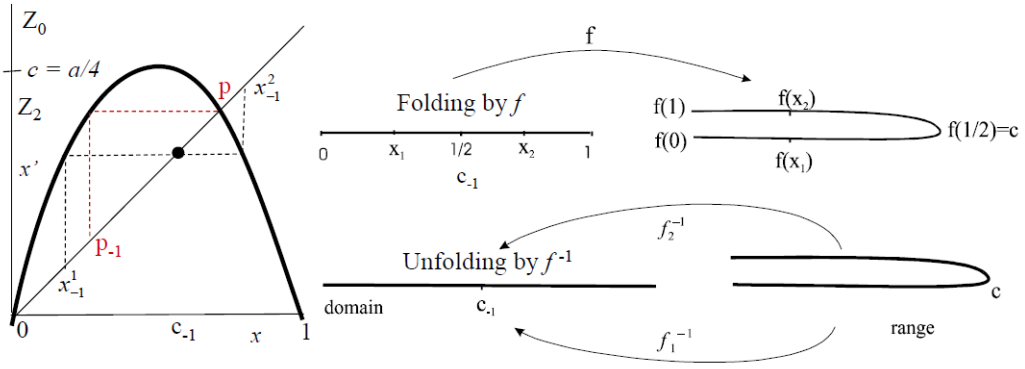

Figure 1.

We remark that in general the condition of vanishing derivative is not sufficient to define the critical points of rank-0 since such condition may be also satisfied by points which are not local extrema (e.g. the inflection points with horizontal tangent). Moreover, for continuous and piecewise differentiable maps the condition of vanishing derivative is not necessary as well, because such maps may have the property that the images of points where the map is not differentiable are critical points, according to the definition given above. This occurs whenever such points are local maxima or minima, like in the cases shown in Figures 2a and 2b. In Figure 2a, a typical $Z_0 - Z_2$ tent map is shown, where the kink point behaves like the critical point of the logistic map even if it is not obtained as image of a point of vanishing derivative. The same reasoning applies to the "bimodal" $Z_1 - Z_3 - Z_1$ piecewise linear function shown in Figure 2b.

The properties of critical points can easily be extended also to piecewise continuous maps T. In this case a point of discontinuity may behave as a critical point of T, even if the definition in terms of merging preimages cannot be applied. This happens when the ranges of the map on the two sides of the discontinuity have an overlapping zone, so that at least one of the two limiting values of the function at the discontinuity separates regions having a different number of rank-1 preimages (see the map shown in Figure 2c, for example). The difference with respect to the case of a continuous map is that now the number of distinct rank-1 preimages through a critical point differs generally by one (instead of two), that is, a critical value c (in general the critical set CS) separates regions Z_k and Z_{k+1}. A one-dimensional example is shown in Figure 2c, where the point of discontinuity is a critical point c_{-1}, and both the two limiting values of the function in c_{-1} are critical points, say c^1 and c^2, associated with c_{-1}, as both c^1 and c^2 separate regions Z_1 and Z_2. Notice that now the critical points have no merging rank-1 preimages. However, the

graph of the $Z_1 - Z_2 - Z_1$ map shown in Figure 2c may be considered as a limiting case of the $Z_1 - Z_3 - Z_1$ obtained. More on the properties and bifurcations of discontinuous maps of the plane can be found in [40].

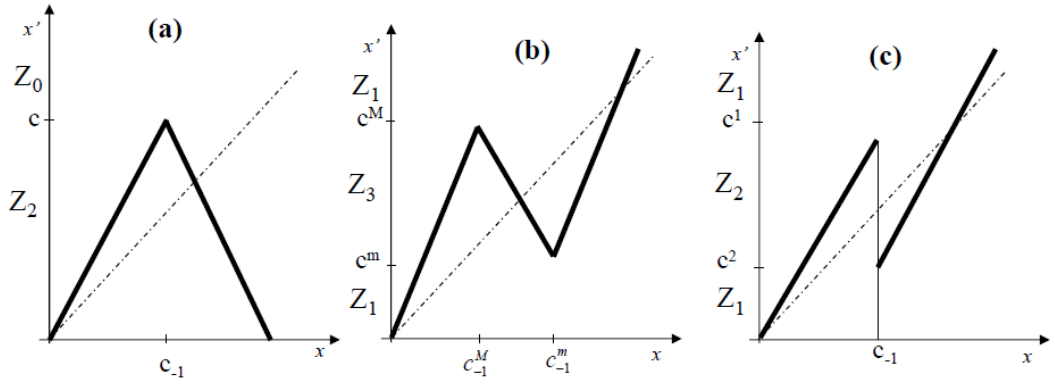

Figure 2.

In order to explain the geometric action of a critical point in a continuous map, let us consider, again, the logistic map, and let us notice that as x moves from 0 to 1 the corresponding image $f(x)$ spans the interval $[0, c]$ twice, the critical point c being the turning point. In other words, if we consider how the segment $\gamma = [0, 1]$ is transformed by the map f, we can say that it is *folded and pleated* to obtain the image $\gamma' = [0, c]$. Such folding gives a geometric reason why two distinct points of γ, say x_1 and x_2, located symmetrically with respect to the point $c_{-1} = 1/2$, are mapped into the same point $x' \in \gamma'$ due to the folding action of f (see Figure 1). The same arguments can be explained by looking at the two inverse mappings f_1^{-1} and f_2^{-1} defined in $(-\infty, a/4]$ according to (3). We can consider the range of the map f formed by the superposition of two half-lines $(-\infty, a/4]$, joined at the critical point $c = a/4$, and on each of these half-lines a different inverse is defined. In other words, instead of saying that two distinct maps are defined on the same half-line we say that the range is formed by two distinct half lines on each of which a unique inverse map is defined. This point of view gives a geometric visualization of the critical point c as the point in which two distinct inverses merge. The action of the inverses, say $f^{-1} = f_1^{-1} \cup f_2^{-1}$, causes an unfolding of the range by mapping c into c_{-1} and by opening the two half-lines one on the right and one on the left of c_{-1}, so that the whole real line $\mathbb{R}$ is covered. So, the map f folds the real line, the two inverses unfold it.

Another interpretation of the folding action of a critical point is the following. Since $f(x)$ is increasing for $x \in [0, 1/2)$ and decreasing for $x \in (1/2, 1]$, its application to a segment $\gamma_1 \subset [0, 1/2)$ is orientation preserving, whereas its application to a segment $\gamma_2 \subset (1/2, 1]$ is orientation reversing. This suggests that an application of f to a segment $\gamma_3 = [a, b]$ including the point $c_{-1} = 1/2$ preserves the orientation of the portion $[a, c_{-1}]$, i.e. $f([a, c_{-1}]) = [f(a), c]$, whereas it reverses the portion $[c_{-1}, b]$, i.e. $f([c_{-1}, b]) = [f(b), c]$, so that $\gamma_3' = f(\gamma_3)$ is folded, the folding point being the critical point c.

Let us now consider the case of a continuous two-dimensional map $T : S \to S$, $S \subseteq \mathbb{R}^2$, defined by

$$T : \begin{cases} x_1' = T_1(x_1, x_2) \\ x_2' = T_2(x_1, x_2) \end{cases}, \tag{4}$$

If we solve the system of the two equations (4) with respect to the unknowns x_1 and x_2, then, for a given (x'_1, x'_2), we may have several solutions, representing rank-1 preimages (or backward iterates) of (x'_1, x'_2), say $(x_1, x_2) = T^{-1}(x'_1, x'_2)$, where T^{-1} is in general a multivalued relation. In this case we say that T is noninvertible, and the critical set (formed by critical curves, denoted by LC from the French "Ligne Critique") constitutes the set of boundaries that separate regions of the plane characterized by a different number of rank-1 preimages. According to the definition, along LC at least two inverses give merging preimages, located on LC_{-1} (Following the notations of [29] and [40]).

For a continuous and (at least piecewise) differentiable noninvertible map of the plane, the set LC_{-1} is included in the set where $\det DT(x_1, x_2)$ changes sign, since T is locally an orientation preserving map near points (x_1, x_2) such that $\det DT(x_1, x_2) > 0$ and orientation reversing if $\det DT(x_1, x_2) < 0$. In order to explain this point, let us recall that when an affine transformation $\mathbf{x}' = A\mathbf{x} + \mathbf{b}$, where $A = \{a_{ij}\}$ is a 2×2 matrix and $\mathbf{b} \in \mathbb{R}^2$, is applied to a plane figure, then the area of the transformed figure grows, or shrinks, by a factor $\rho = |\det A|$, and if $\det A > 0$ then the orientation of the figure is preserved, whereas if $\det A < 0$ then the orientation is reversed. This property also holds for the linear approximation of (4) in a neighborhood of a point $\mathbf{p} = (x_1, x_2)$, given by an affine map with $A = DT$, DT being the Jacobian matrix evaluated at the point $\mathbf{p}$

$$DT(\mathbf{p}) = \begin{pmatrix} \partial T_1/\partial x_1 & \partial T_1/\partial x_2 \\ \partial T_2/\partial x_1 & \partial T_2/\partial x_2 \end{pmatrix} (\mathbf{p}) \,. \tag{5}$$

A qualitative visualization is given in Figure 3. Of course, if the map is continuously differentiable then the change of the sign of DT occurs along points where DT vanishes, thus giving the characterization of the fold line LC_{-1} as the locus where the jacobian vanishes.

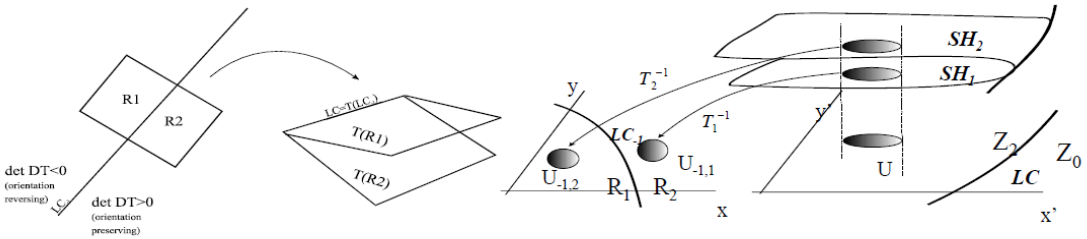

Figure 3.

In order to give a geometrical interpretation of the action of a multi-valued inverse relation T^{-1}, it is useful to consider a region Z_k as the superposition of k sheets, each associated with a different inverse. Such a representation is known as *Riemann foliation* of the plane (see e.g. [40]). Different sheets are connected by folds joining two sheets, and the projections of such folds on the phase plane are arcs of LC. This is shown in the qualitative sketch of Figure 3 (right), where the case of a $Z_0 - Z_2$ noninvertible map is considered. This graphical representation of the unfolding action of the inverses also gives an intuitive idea of the mechanism which causes the creation of non-connected basins for noninvertible maps of the plane.

To give an example, let us again consider a quadratic map $T : (x, y) \to (x', y')$, extensively studied in [40], see also [3], defined by

$$T : \begin{cases} x' = ax + y \\ y' = b + x^2 \end{cases} \tag{6}$$

Given x' and y', if we try to solve the algebraic system with respect to the unknowns x and y we get two solutions, given by

$$T_1^{-1} : \begin{cases} x = -\sqrt{y' - b} \\ y = x' + a\sqrt{y' - b} \end{cases} \quad ; \qquad T_2^{-1} : \begin{cases} x = \sqrt{y' - b} \\ y = x' - a\sqrt{y' - b} \end{cases} \tag{7}$$

if $y' \geq b$, and no solutions if $y' < b$. So, (6) is a $Z_0 - Z_2$ noninvertible map, where Z_0 (region whose points have no preimages) is the half plane $Z_0 = \{(x, y) \,|y < b\}$ and Z_2 (region whose points have two distinct rank-1 preimages) is the half plane $Z_2 = \{(x, y) \,|y > b\}$. The line $y = b$, which separates these two regions, is LC, i.e. the locus of points having two merging rank-1 preimages, located on the line $x = 0$, that represents LC_{-1}. Being (6) a continuously differentiable map, the points of LC_{-1} necessarily belong to the set of points at which the Jacobian determinant vanishes, i.e. $LC_{-1} \subseteq J_0$, where $J_0 = \{(x, y) \,|\, \det DT(x, y) = -2x = 0\}$. In this case LC_{-1} coincides with J_0 (the vertical axis $x = 0$) and the critical curve LC is the image by T of LC_{-1}, i.e. $LC = T(LC_{-1}) = T(\{x = 0\}) = \{(x, y) \,|y = b\}$.

In order to show the folding action related to the presence of the critical lines fact, we consider a plane figure (a circle) U separated by LC_{-1} into two portions, say $U_1 \in R_1$ and $U_2 \in R_2$ (Figure 4a) and we apply the map (6) to the points of U. The image $T(U_1) \cap T(U_2)$ is a nonempty set included in the region Z_{k+2}, which is the region whose points p' have rank-1 preimages $p_1 = T_1^{-1}(p') \in U_1$ and $p_2 = T_2^{-1}(p') \in U_2$. This means that two points $p_1 \in U_1$ and $p_2 \in U_2$, located at opposite sides with respect to LC_{-1}, are mapped in the same side with respect to LC, in the region Z_{k+2}. This is also expressed by saying that the ball U is "folded" by T along LC on the side with more preimages (see Figure 4). The same concept can be equivalently expressed by stressing the "unfolding" action of T^{-1}, obtained by the application of the two distinct inverses in Z_{k+2} which merge along LC. Indeed, if we consider a ball $V \subset Z_{k+2}$, then the set of its rank-1 preimages $T_1^{-1}(V)$ and $T_2^{-1}(V)$ is made up of two balls $T_1^{-1}(V) \in R_1$ and $T_2^{-1}(V) \in R_2$. These balls are disjoint if $V \cap LC = \emptyset$ (Figure 4b).

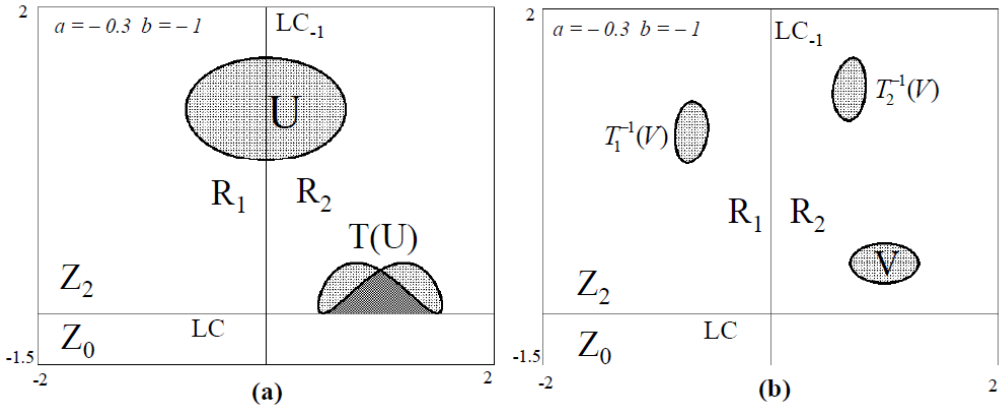

Figure 4.

Many of the considerations made above, for 1-dimensional and 2-dimensional noninvertible maps, can be generalized to n-dimensional ones, even if their visualization becomes and in particular the visualization of the contacts involved becomes more difficult (see e.g. [19] and [22]). In any case, the importance of the critical sets CS lies in the fact that their points separate regions Z_k characterized by different number of preimages.

2.2 Discrete dynamical system as iterated maps

A *discrete-time dynamical system*, defined by the difference equation (1) can be seen as the result of the repeated application (or *iteration*) of the map T. Indeed, the point $\mathbf{x}$ represents the state of a system, and T represents the "unit time advancement operator" $T : \mathbf{x}_t \to \mathbf{x}_{t+1}$. Starting from an *initial condition* $\mathbf{x}_0 \in S$, the iteration of T inductively defines a unique *trajectory*

$$\tau(\mathbf{x}_0) = \left\{ \mathbf{x}_t = T^t(\mathbf{x}_0), t = 0, 1, 2, \dots \right\}, \tag{8}$$

where T^0 is the identity map and $T^t = T(T^{t-1})$. As $t \to +\infty$, a trajectory may diverge, or it may converge to a fixed point of the map T, i.e. a point $\overline{\mathbf{x}}$ such that $T(\overline{\mathbf{x}}) = \overline{\mathbf{x}}$, or it may asymptotically approach another kind of invariant set, such as a periodic cycle, or a closed invariant curve or a more complex attractor, for example a so called chaotic attractor ([24, 28]). We recall that a set $A \subset \mathbb{R}^2$ is *invariant* for the map T if it is mapped onto itself, $T(A) = A$. This means that if $x \in A$ then $T(x) \in A$, i.e. A is *trapping,* and every point of A is image of some point of A. A closed invariant set A is an *attractor* if (i) it is *Lyapunov stable,* i.e. for every neighborhood W of A there exists a neighborhood V of A such that $T^t(V) \subset W$ for all $t \geq 0$; (ii) a neighborhood U of A exists such that $T^t(\mathbf{x}) \to A$ as $t \to +\infty$ for each $\mathbf{x} \in U$.

The *basin of an attractor* A is the set of all points that generate trajectories converging to A

$$\mathcal{B}(A) = \left\{ \mathbf{x} | T^t(\mathbf{x}) \to A \quad \text{as } t \to +\infty \right\} \tag{9}$$

Let $U(A)$ be a neighborhood of an attractor A whose points converge to A. Of course $U(A) \subseteq \mathcal{B}(A)$, and also the points that are mapped into U after a finite number of iterations belong to $\mathcal{B}(A)$. Hence, the basin of A is given by

$$\mathcal{B}(A) = \bigcup_{n=0}^{\infty} T^{-n}(U(A)) \tag{10}$$

where $T^{-1}(\mathbf{x})$ represents the set of the rank-1 preimages of $\mathbf{x}$ (i.e. the points mapped into $\mathbf{x}$ by T), and $T^{-n}(\mathbf{x})$ represents the set of the rank-n preimages of $\mathbf{x}$ (i.e. the points mapped into $\mathbf{x}$ after n applications of T).

Let $\mathcal{B}$ be a basin of attraction and $\partial\mathcal{B}$ its boundary. From the definition it follows that $\mathcal{B}$ is trapping with respect to the forward iteration of the map T and invariant with respect to the backward iteration of all the inverses T^{-1}. Points belonging to $\partial\mathcal{B}$ are mapped into $\partial\mathcal{B}$ both under forward and backward iteration of T. This implies that if an unstable fixed point or cycle belongs to $\partial\mathcal{B}$ then $\partial\mathcal{B}$ must also contain all of its preimages of any rank. Moreover, if a saddle-point, or a saddle-cycle, belongs to $\partial\mathcal{B}$, then $\partial\mathcal{B}$ must also contain the whole stable set (see [29] and [40]).

A problem that often arises in the study of nonlinear dynamical systems concerns the existence of several attracting sets, each with its own basin of attraction. In this case the dynamic process becomes path-dependent, i.e. which kind of long run dynamics characterizes the system depends

on the starting condition. Another important problems in the study of applied dynamical systems is the delimitation of a bounded region of the state space where the system dynamics are ultimately trapped, despite of the complexity of the long-run time patterns. This is an useful information, even more useful than a detailed description of step by step time evolution.

Both these questions require an analysis of the global dynamical properties of the dynamical system, that is, an analysis which is not based on the linear approximation of the map. When the map T is noninvertible, its global dynamical properties can be usefully characterized by using the formalism of critical sets, by which the folding action associated with the application of the map, as well as the "unfolding" associated with the action of the inverses, can be described. Loosely speaking, the repeated application of a noninvertible map repeatedly folds the state space along the critical sets and their images, and often this allows one to define a bounded region where asymptotic dynamics are trapped. As some parameter is varied, global bifurcations that cause sudden qualitative changes in the properties of the attracting sets can be detected by observing contacts of critical curves with invariant sets. Instead, the repeated application of the inverses "repeatedly unfold" the state space, so that a neighborhood of an attractor may have preimages far from it, thus giving rise to complicated topological structures of the basins, that may be formed by the union of several (even infinitely many) non connected portions. In fact, from (10) it follows that in order to study the extension of a basin and the structure of its boundaries one has to consider the properties of the inverse relation T^{-1}. The route to more and more complex basin boundaries, as some parameter is varied, is characterized by global bifurcations, also called contact bifurcations, due to contacts between the critical set and the invariant sets that form the basins' boundaries.

2.3 Critical sets and the delimitation of trapping regions.

Portions of the critical set CS and its images $CS_k = T^k(CS)$ can be used to obtain the boundaries of trapping regions where the asymptotic dynamics of the iterated points of a noninvertible map are confined. This can be easily explained for a one-dimensional noninvertible map, for example the quadratic map (2). In fact, it is quite evident that if we iterate the logistic map for $3 < \mu < 4$ starting from an initial condition inside the interval $[c_1, c]$, with $c_1 = f(c)$, no images can be obtained out of this interval (see Figure 5), i.e. the interval formed by the critical point c and its rank-1 image c_1 is trapping. Moreover, any trajectory generated from an initial condition in $(0, 1)$, enters $[c_1, c]$ after a finite number of iterations. Following the terminology introduced in [40], the interval $[c_1, c]$ is called *absorbing*.

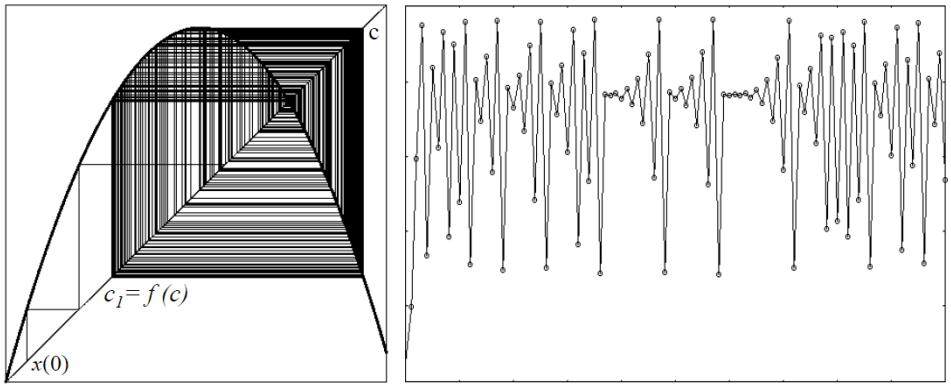

Figure 5.

In general, for an n-dimensional map, an *absorbing region* $\mathcal{A}$ *(intervals in R, areas in* R^2*, volumes in* R^3*, ...)* is defined as a bounded set whose boundary is given by portions of the critical set CS and its images of increasing order $CS_k = T^k(CS)$, such that a neighborhood $U \supset \mathcal{A}$ exists whose point enter $\mathcal{A}$ after a finite number of iterations and then never escape it, since $T(\mathcal{A}) \subseteq \mathcal{A}$, i.e. $\mathcal{A}$ is trapping (see [40] for more details).

Loosely speaking, we can say that the iterated application of a noninvertible map, folding and folding again the space, defines trapping regions bounded by critical sets of increasing order.

Sometimes, smaller absorbing regions are nested inside a bigger one. This can be illustrated, again, for the logistic map (2), as shown in Figure 6a, where inside the absorbing interval $[c_1, c]$ a trapping subset is obtained by higher rank images of the critical point, given by $\mathcal{A} = [c_1, c_3] \cup [c_2, c]$. In Figure 6b it is shown that, for the same parameter value $\mu = 3.61$ as in Figure 6a, the numerical iteration of the logistic map gives points which are trapped inside the two-cyclic interval $\mathcal{A}$.

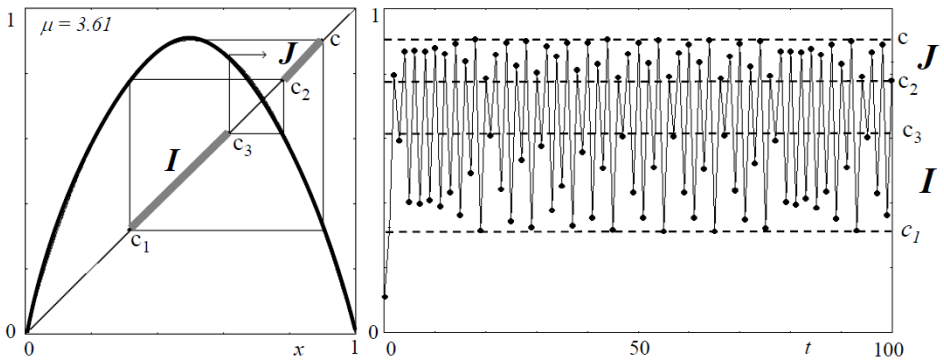

Figure 6.

Inside an absorbing region one or more attractors may exist. However, if a chaotic attractor exists which fills up a whole absorbing region then boundary of the chaotic attractor is formed by portions of critical sets.

This is the situation shown in Figure 6, where the absorbing interval $\mathcal{A} = [c_1, c_3] \cup [c_2, c]$ is invariant and filled up by a chaotic trajectory, as shown in Figure 6b. To better illustrate this point, we also give a two-dimensional example, obtained by using the map (6). In Figure 7a chaotic trajectory is shown, and in Figure 7b its outer boundary is obtained by the union of a segment of LC and three iterates $LC_i = T^i(LC)$, $i = 1, 2, 3$.

Indeed, following [40] (see also [10]) a practical procedure can be outlined in order to obtain the boundary of an absorbing area (although it is difficult to give a general method). Starting from a portion of LC_{-1}, approximately taken in the region occupied by the area of interest, its images by T of increasing rank are computed until a closed region is obtained. When such a region is mapped into itself, then it is an absorbing area $\mathcal{A}$. The length of the initial segment is to be taken, in general, by a trial and error method, although several suggestions are given in the books referenced above. Once an absorbing area $\mathcal{A}$ is found, in order to see if it is invariant or not the same procedure must be repeated by taking only the portion$\gamma = \mathcal{A} \cap LC_{-1}$ as the starting segment. Then, one of the following two cases occurs:

Case I: the union of m iterates of γ (for a suitable m) covers the whole boundary of $\mathcal{A}$; in which case $\mathcal{A}$ is an invariant absorbing area, and

$$\partial\mathcal{A} \subset \bigcup_{k=1}^{m} T^k(\gamma) \tag{11}$$

Case II: no natural m exists such that $\bigcup_{i=1}^{m} T^i(\gamma)$ covers the whole boundary of $\mathcal{A}$; in which case $\mathcal{A}$ is not invariant but strictly mapped into itself. An invariant absorbing area is obtained by $\cap_{n>0} T^n(\mathcal{A})$ (and may be obtained by a finite number of images of $\mathcal{A}$).

The application of this procedure to the problem of the delimitation of the chaotic area of Figure 7a by portions of critical curves suggests us, on the basis of Figure 7b, to take a smaller segment γ and to take an higher number of iterates in order to obtain also the inner boundary. The result is shown in Figure 8a, where by four iterates we get the outer boundary. By a few more iterates also the inner boundary of the chaotic area is get, as shown in Figure 8b. As it can be clearly seen, and as clearly expressed by the strict inclusion in (11), the union of the images also include several arcs internal to the invariant area $\mathcal{A}$. Indeed, the images of the critical arcs which are mapped inside the area play a particular role, because these curves represent the "foldings" of the plane under forward iterations of the map, and this is the reason why these inner curves often denote the portions of the region which are more frequently visited by a generic trajectory inside it (compare Figure 7a with Figure 8b). Many examples are given in the literature on noninvertible maps, see [40] for example. This is due to the fact that points close to a critical arc LC_i, $i \geq 0$, are more frequently visited, because there are several distinct parts of the invariant area which are mapped in the same region (close to LC_i) in $i+1$ iterations.

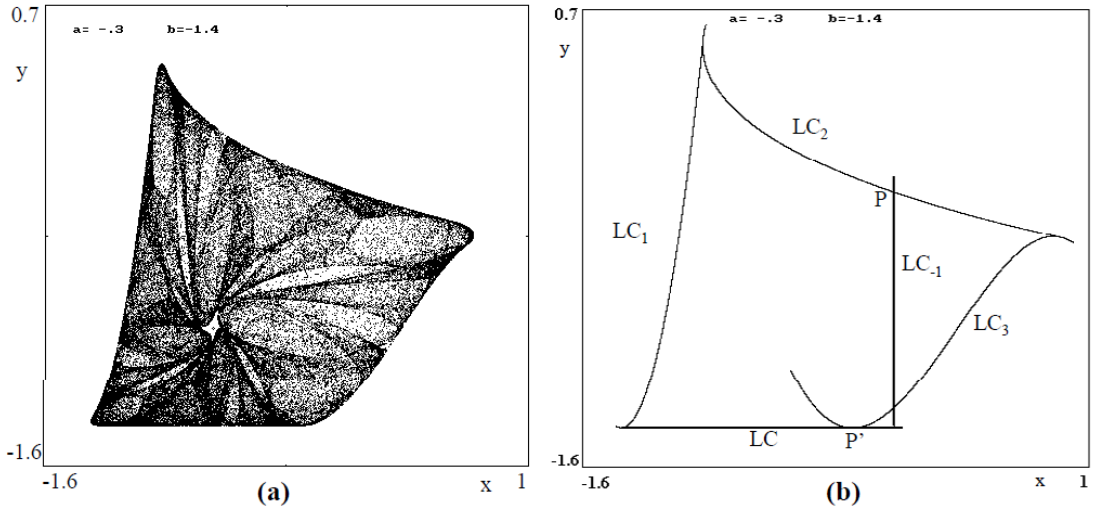

Figure 7.

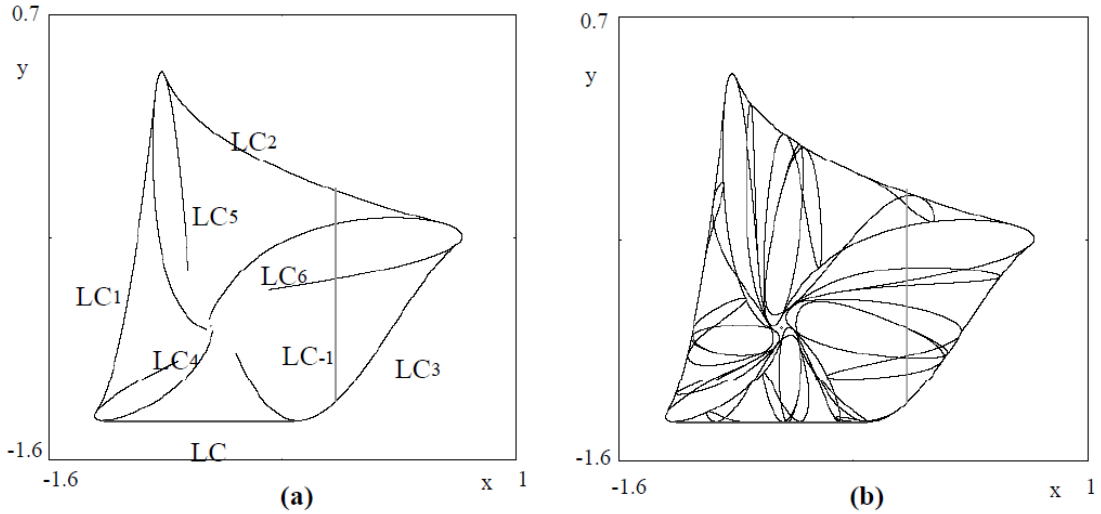

Figure 8.

2.4 Critical sets and the creation of non connected basins

From (10) it is clear that the properties of the inverses are important in order to understand the structure of the basins and the main bifurcations which change their qualitative properties. In the case of noninvertible maps, the multiplicity of preimages may lead to basins with complex structures, such as multiply connected or non connected sets, sometimes formed by infinitely many non connected portions. In the context of noninvertible maps it is useful to define the *immediate basin* $\mathcal{B}_0(A)$, of an attracting set A, as the widest connected component of the basin which contains A. Then the total basin can be expressed as

$$\mathcal{B}(A) = \bigcup_{n=0}^{\infty} T^{-n}(\mathcal{B}_0(A))$$

where $T^{-n}(\mathbf{x})$ represents the set of all the rank-n preimages of x, i.e. the set of points which are mapped in $\mathbf{x}$ after n iterations of the map T. The backward iteration of a noninvertible map *repeatedly unfolds* the phase space, and this implies that the basins may be non-connected, i.e. formed by several disjoint portions.

Also in this case, we first illustrate this property by using a one-dimensional map[2] In Figure 9 the graph of a $Z_1 - Z_3 - Z_1$ noninvertible map is shown, where Z_3 is the portion of the codomain bounded by the relative minimum value $c_{\min}$ and relative maximum value $c_{\max}$. In the situation shown in Figure 9a we have three attractors: the fixed point z^*, with $\mathcal{B}(z^*) = (-\infty, q^*)$, the attractor A around x^*, with basin $\mathcal{B}(A) = (q^*, r^*)$ bounded by two unstable fixed points, and $+\infty$ (i.e. positively diverging trajectories) with basin $\mathcal{B}(+\infty) = (r^*, +\infty)$. In this case all the basins are immediate basins, each being given by an open interval. In the situation shown in Figure 9a, both basin boundaries q^* and r^* are in Z_1, so they have only themselves as unique preimages (like for an invertible map). However, the situation drastically changes if, for example, some parameter changes causes the minimum value $c_{\min}$ to move downwards, until it goes below

[2]The example is taken from an evolutionary game proposed in [8].

q^* (as in Figure 9b). After the global bifurcation, when $c_{\min} = q^*$, the portion $(c_{\min}, q^*)$ enters Z_3, so new preimages $f^{-k}(c_{\min}, q^*)$ appear with $k \geq 1$. These preimages constitute an infinite (countable) set of non-connected portions of $\mathcal{B}(z^*)$ nested inside $\mathcal{B}(A)$, represented by the thick portions of the diagonal in Figure 9b, bounded by the infinitely many preimages of any rank, say q^*_{-k}, $k \in \mathbb{N}$, of q^*, that accumulate in a left neighborhood of the fixed point r^*. In fact, as r^* is a repelling fixed point for the forward iteration of f, it is an attracting fixed point for the backward iteration of the same map.. So, the contact between the critical point $c_{\min}$ and the basin boundary q^* marks the transition from simple connected to non connected basins. Similar global bifurcations, due to contacts between critical sets and basin boundaries, also occur in higher dimensional maps.

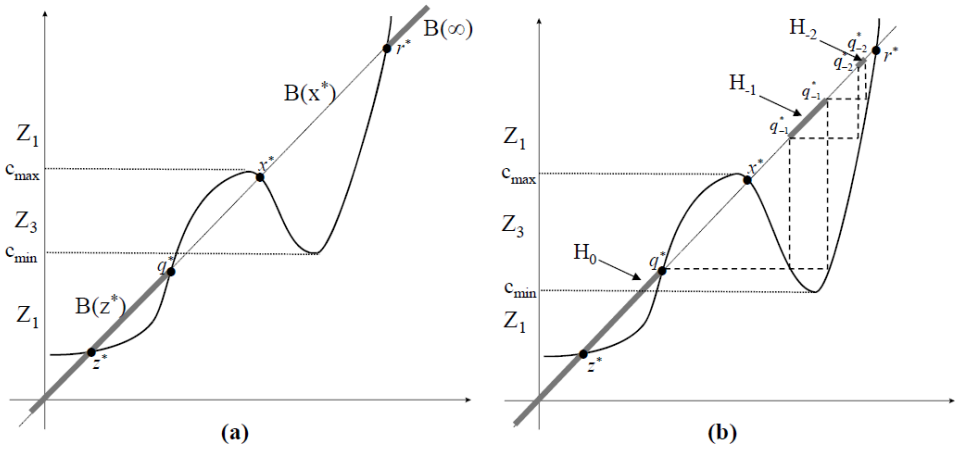

Figure 9.

Also in higher dimensional cases, the global bifurcations which give rise to complex topological structures of the basins, like those formed by non connected sets, can be explained in terms of contacts of basins boundaries and critical sets. In fact, if a parameter variation causes a crossing between a basin boundary and a critical set which separates different regions Z_k so that a portion of a basin enters a region where an higher number of inverses is defined, then new components of the basin may suddenly appear at the contact. However, for maps of dimension greater than 1, such kinds of bifurcations can be very rarely studied by analytical methods, since the analytical equations of such singularities are not known in general. Hence such studies are mainly performed by geometric and numerical methods.

Several examples of two-dimensional noninvertible maps that have non connected basins can be found in [38, 39] and [40] (see also [3, 8, 12], and [17], for several applications to the modeling of economic and social systems). The following example is taken from [17], where the time evolution of a duopoly game is modeled by the iteration of the following two-dimensional noninvertible map:

$$\begin{aligned} x' &= (1-\alpha_1)\, x + \alpha_1 \mu_1 y\,(1-y) \\ y' &= (1-\alpha_2)\, y + \alpha_2 \mu_2 x\,(1-x) \end{aligned} \tag{12}$$

Under the assumption $\mu_1 = \mu_2 = \mu$, the fixed points can be expressed by simple analytical expressions: besides the trivial solution $O = (0, 0)$, a positive symmetric equilibrium exists for

$\mu > 1$, given by $S = ((\mu-1)/\mu, (\mu-1)/\mu)$. Two further equilibria $E_1 = (\bar{x}, \bar{y})$ and $E_2 = (\bar{y}, \bar{x})$ exist for $\mu > 3$, where $\bar{x} = \left(\mu + 1 + \sqrt{\psi}\right)/2\mu$, $\bar{y} = \left(\mu + 1 - \sqrt{\psi}\right)/2\mu$ with $\psi = (\mu + 1)(\mu - 3)$. These equilibria are located in symmetric positions with respect to the diagonal $y = x$. As shown in [17], a wide range of parameters μ, α_1, α_2 exists such that E_1 and E_2 are both stable. Accordingly, a problem of equilibrium selection arises, which leads to the question of the delimitation of the two basins of attraction $\mathcal{B}(E_1)$ and $\mathcal{B}(E_2)$.

As argued above, the properties of the inverses of the map become important in order to understand the structure of the basins and their qualitative changes. Indeed, the map (12) is a noninvertible map, because a point $(x', y') \in \mathbb{R}^2$ may have up to four rank-1 preimages, that can be computed by solving the fourth degree algebraic system (12) with respect to x and y. The critical curves are computed as follows: LC_{-1} coincides with the set of points in which the Jacobian determinant vanishes, i.e. $\det DT = 0$, where

$$DT(x, y) = \begin{bmatrix} 1 - \alpha_1 & \alpha_1\mu_1(1 - 2y) \\ \alpha_2\mu_2(1 - 2x) & 1 - \alpha_2 \end{bmatrix} \tag{13}$$

and $LC = T(LC_{-1})$. So, LC_{-1} is an equilateral hyperbola, of equation

$$\left(x - \frac{1}{2}\right)\left(y - \frac{1}{2}\right) = \frac{(1 - \alpha_1)(1 - \alpha_2)}{4\alpha_1\alpha_2\mu_1\mu_2}. \tag{14}$$

Since LC_{-1} is formed by the union of two disjoint branches, say $LC_{-1} = LC_{-1}^{(a)} \cup LC_{-1}^{(b)}$, it follows that also $LC = T(LC_{-1})$ is the union of two branches, say $LC^{(a)} = T(LC_{-1}^{(a)})$ and $LC^{(b)} = T(LC_{-1}^{(b)})$, see Figure 10. The branch $LC^{(a)}$ separates the region Z_0, whose points have no preimages, from the region Z_2, whose points have two distinct rank-1 preimages. The other branch $LC^{(b)}$ separates the region Z_2 from Z_4, whose points have four distinct preimages. Any point of $LC^{(a)}$ has two coincident rank-1 preimages, located at a point of $LC_{-1}^{(a)}$, and any point of $LC^{(b)}$ has two coincident rank-1 preimages, located at a point of $LC_{-1}^{(b)}$, plus two further distinct rank-1 preimages, called *extra preimages*. Following the terminology of [40], we say that the map (12) is a noninvertible map of $Z_4 > Z_2 - Z_0$ type, where the symbol "$>$" denotes the presence of a cusp point in the branch $LC^{(b)}$ (see Figure 10, where the corresponding *Riemann foliation* is shown as well. Different sheets are connected by folds joining two sheets, and the projections of such folds on the phase plane are arcs of LC. The cusp point of LC is characterized by three merging preimages at the junction of two folds.

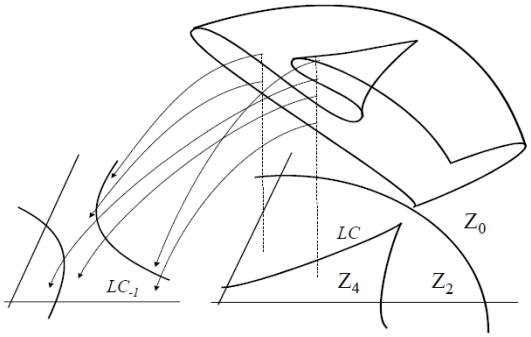

Figure 10.

In order to study the structure of the basins and explain the global bifurcations that change their qualitative properties, we first consider the symmetric case of players with homogeneous expectations, i.e. $\alpha_1 = \alpha_2 = \alpha$. In this case, the map (12) has a symmetry property, as it remains the same if the variables x and y are swapped. Formally, we have $T(P(x,y)) = P(T(x,y))$, where $P : (x,y) \to (y,x)$ is the reflection through the diagonal $\Delta = \{(x,x), x \in \mathbb{R}\}$. This symmetry property implies that the diagonal Δ is a trapping subspace for the map T, i.e. $T(\Delta) \subseteq \Delta$. The trajectories embedded in Δ are governed by the restriction of the two-dimensional map T to Δ, i.e. $f = T|_\Delta : \Delta \to \Delta$. The map f, obtained by setting $x = y$ and $x' = y'$ in (12), is given by $x' = f(x) = (1 + \alpha(\mu - 1))\, x - \alpha\mu x^2$. In the symmetric case of homogeneous players we can give a complete analytical characterization of the global bifurcation that transforms the basins from simply connected sets to multiply connected. In fact, the following result is given in [17]:

If $\mu_1 = \mu_2 = \mu$ and $\alpha_1 = \alpha_2 = \alpha$ and the equilibria E_1 and E_2 are both stable, then the common boundary $\partial\mathcal{B}(E_1) \cap \partial\mathcal{B}(E_2)$ which separates the basin $\mathcal{B}(E_1)$ from the basin $\mathcal{B}(E_2)$ is given by the stable set $W^s(S)$ of the saddle point S. If $\alpha(\mu+1) < 1$ then $W^s(S) = OO_{-1}^{(1)}$, where $O = (0,0)$ and $O_{-1}^{(1)} = \left(\frac{1+\alpha(\mu-1)}{\alpha\mu}, \frac{1+\alpha(\mu-1)}{\alpha\mu}\right)$, and the two basins are simply connected sets. If $\alpha(\mu+1) > 1$ then the two basins are non-connected sets, formed by infinitely many simply connected components.

The bifurcation occurring at $\alpha(\mu+1) = 1$ is a *global bifurcation*. It cannot be revealed by a study of the linear approximation of the dynamical system and the occurrence of such a bifurcation can be characterized by a contact between the stable set of the symmetric fixed point S and a critical curve. In order to explain this, we start from a set of parameters such that both of the basins are simply connected, like in Figure 11a, where $\mu_1 = \mu_2 = \mu = 3.4$ and $\alpha_1 = \alpha_2 = \alpha = 0.2 < 1/(\mu+1)$. For this set of parameters, four fixed points exist, indicated by O, S, E_1 and E_2. The fixed points O and S are saddle points, whereas the equilibria E_1 and E_2 are both stable, each with its own basin of attraction. These basins, $\mathcal{B}(E_1)$ and $\mathcal{B}(E_2)$, are represented by white and light grey respectively (the dark grey region represents the set of initial conditions which generate unbounded trajectories; we could refer to this set as the basin of infinity).

Now let us turn to an explanation of the global bifurcation which causes the transition between these rather different structures of the basins. First notice that the boundary separating $\mathcal{B}(E_1)$ and $\mathcal{B}(E_2)$ contains the symmetric equilibrium S as well as its whole stable set $W^s(S)$. In fact, just after the creation of the two stable fixed points E_1 and E_2 for $\mu = 3$, the symmetric equilibrium $S \in \Delta$ is a saddle point. The two branches of the unstable set $W^u(S)$ departing from it reach E_1 and E_2 respectively. Hence, since a basin boundary is backward invariant (see [38] and [40]), not only the local stable set $W^s_{loc}(S)$ belongs to the boundary that separates the two basins, but also its preimages of any rank: $W^s(S) = \bigcup_{k\geq 0} T^{-k}(W^s_{loc}(S))$. Because of the symmetry property of the system (12) with homogeneous players, the local stable set of S belongs to the invariant diagonal Δ. As long as $\alpha(\mu+1) < 1$, the whole stable set $W^s(S)$ belongs to Δ and is given by $W^s(S) = OO_{-1}^{(1)}$, where $O_{-1}^{(1)}$ is the preimage of O located along Δ. Observe that if $\alpha(\mu+1) < 1$ holds, the cusp point K of the critical curve $LC^{(b)}$ has negative coordinates and, consequently, the whole segment $OO_{-1}^{(1)}$ belongs to the regions Z_0 and Z_2, see Figure 11a. This implies that the two preimages of any point of $OO_{-1}^{(1)}$ belong to Δ (they can be computed by the restriction f of T to the invariant diagonal Δ). This proves that the segment $OO_{-1}^{(1)}$ is backward invariant, i.e. it includes all its preimages. The structure of the basins $\mathcal{B}(E_i)$, $i = 1, 2$, is very simple: $\mathcal{B}(E_1)$ is entirely located below the diagonal Δ and $\mathcal{B}(E_2)$ is entirely located above it. Both of the basins

$\mathcal{B}(E_1)$ and $\mathcal{B}(E_2)$ are simply connected sets.

Their structure becomes a lot more complex for $\alpha(\mu+1) > 1$. In order to understand the bifurcation occurring at $\alpha(\mu+1) = 1$, we consider the critical curves of the map (12). At $\alpha(\mu+1) = 1$ a contact between $LC^{(b)}$ and the fixed point O occurs, due to the merging between O and the cusp point K.[3] For $\alpha(\mu+1) > 1$, the portion KO of $W^S_{loc}(S)$ belongs to the region Z_4, where four inverses of T exist. This implies that besides the two rank-1 preimages on Δ, the points of KO have two further preimages, which are located on the segment $O^{(2)}_{-1}O^{(3)}_{-1}$ of the line Δ_{-1}. Since $OO^{(1)}_{-1} = W^s_{loc}(S) \subset \partial\mathcal{B}(E_1) \cap \partial\mathcal{B}(E_2)$, also its preimages of any rank belong to the boundary which separates $\mathcal{B}(E_1)$ from $\mathcal{B}(E_2)$. So the rank-1 preimages of the segment $O^{(2)}_{-1}O^{(3)}_{-1}$, which exist because portions of it are included in the regions Z_2 and Z_4, belong to $W^s(S)$ as well, being preimages of rank-2 of $OO^{(1)}_{-1}$. This repeated procedure, based on the iteration of the multi-valued inverse of T, leads to the construction of the whole stable set $W^s(S)$.

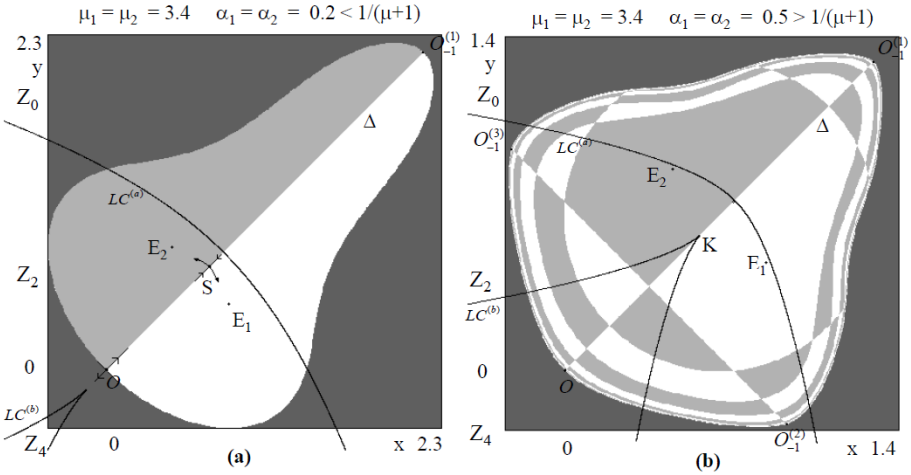

Figure 11.

Similar results can be obtained in the case $\alpha_1 \neq \alpha_2$. The main difference with respect to the homogeneous case lies in the fact that the diagonal Δ is no longer invariant. Even if the fixed points remain the same, the basins are no longer symmetric with respect to Δ. Nevertheless, many of the arguments given above continue to hold in the case of heterogeneous beliefs. In particular, the boundary which separates the basin of equilibrium E_1 from that of E_2 is still formed by the whole stable set $W^s(S)$, but in the case $\alpha_1 \neq \alpha_2$ the local stable set $W^s_{loc}(S)$ is not along the diagonal Δ. The contact between $W^s(S)$ and $LC^{(b)}$, which causes the transition from simple to complex basins, does not occur at O (since now $O \notin W^s(S)$) and no longer involves the cusp point of $LC^{(b)}$. So, the parameter values at which such contact bifurcations occur cannot be computed analytically.

[3] To compute the coordinates of the cusp point of $LC^{(b)}$ notice that in any point of LC_{-1} at least one eigenvalue of DT vanishes. In the point $C_{-1} = LC^{(a)}_{-1} \cap \Delta = (c_{-1}, c_{-1})$, with $c_{-1} = (\alpha(\mu-1)+1)/2\alpha\mu$, the eigenvalue $z_{\|}$ with eigendirection along Δ vanishes, and its image $C = LC^{(a)} \cap \Delta = (c, c)$ with $c = f(c_{-1}) = (\alpha(\mu-1)+1)^2/4\alpha\mu$ is the point at which $LC^{(a)}$ intersects Δ. This corresponds to the unique critical point of the restriction of T to Δ. At the other intersection of LC_{-1} with Δ, given by $K_{-1} = LC^{(b)}_{-1} \cap \Delta = (k_{-1}, k_{-1})$ with $k_{-1} = (\alpha(\mu-1)-1)/2\alpha\mu$ the eigenvalue $z_{\perp}$ vanishes, and the curve $LC^{(b)} = T(LC^{(b)}_{-1})$ has a *cusp point* $K = LC^{(b)} \cap \Delta = (k, k)$ with $k = f(k_{-1}) = (\alpha(\mu+1)-1)(\alpha\mu+3(1-\alpha))/4\alpha\mu$.

In Figure 12a, obtained with $\mu = 3.6$, $\alpha_1 = 0.55$ and $\alpha_2 = 0.7$, the two equilibria E_1 and E_2 are stable, and their basins are connected sets. An asymmetry in the expectation formation process has a negligible effect on the local stability properties of the equilibria, but it results in an evident asymmetry in the basins of attraction. As shown in Figure 11a, when $\alpha_2 > \alpha_1$ the extension of $\mathcal{B}(E_2)$ is, in general, greater than the extension of $\mathcal{B}(E_1)$.

Moreover, the situation is not always as simple as in Figure 12a. The symmetric equilibrium S is a saddle fixed point and is included in the boundary – the whole stable set $W^s(S)$ – which separates the two basins. It can be noticed that in the simple situation shown in Figure 12a, the whole stable set $W^s(S)$ is entirely included inside the regions Z_2 and Z_0. However, the fact that a portion of $W^s(S)$ is close to LC suggests that a contact bifurcation may occur if, e.g., the adjustment coefficients are slightly changed. In fact, if a portion of $\mathcal{B}(E_1)$ enters Z_4 after a contact with $LC^{(b)}$, new rank-1 preimages of that portion will appear near $LC_{-1}^{(b)}$. This is the situation illustrated in Figure 12b, obtained after a small change of α_1. The portion of $\mathcal{B}(E_1)$ inside Z_4 is denoted by H_0. It has two rank-1 preimages, denoted by $H_{-1}^{(1)}$ and $H_{-1}^{(2)}$, which are located at opposite sides with respect to $LC_{-1}^{(b)}$ and merge on it (by definition the rank-1 preimages of the arc of $LC^{(b)}$ which bound H_0 must merge along $LC_{-1}^{(b)}$). The set $H_{-1} = H_{-1}^{(1)} \cup H_{-1}^{(2)}$ constitute a non-connected portion of $\mathcal{B}(E_1)$. Moreover, since H_{-1} belongs to the region Z_4, it has four rank-1 preimages, denoted by $H_{-2}^{(j)}$, $j = 1, ..., 4$ in Figure 10b, which constitute other four "islands"[4] of $\mathcal{B}(E_1)$. Points of these "islands" are mapped into H_0 after two iterations of the map T. Indeed, infinitely many higher rank preimages of H_0 exist, thus giving infinitely many smaller and smaller disjoint "islands" of $\mathcal{B}(E_1)$. Hence, at the contact between $W^s(S)$ and LC, the basin $\mathcal{B}(E_1)$ is transformed from a simply connected into a non-connected set, constituted by infinitely many disjoint components. The larger connected component of $\mathcal{B}(E_1)$ which contains E_1 is the *immediate basin* $\mathcal{B}_0(E_1)$, and the whole basin is given by the union of the infinitely many preimages of $\mathcal{B}_0(E_1)$: $\mathcal{B}(E_1) = \bigcup_{k\geq 0} T^{-k}(\mathcal{B}_0(E_1))$. Observe that even if small differences between the adjustment speeds have negligible effects on the properties of the attractors, they may cause remarkable asymmetries in the structure of the basins, which can only be detected when the global properties of the economic model are studied.

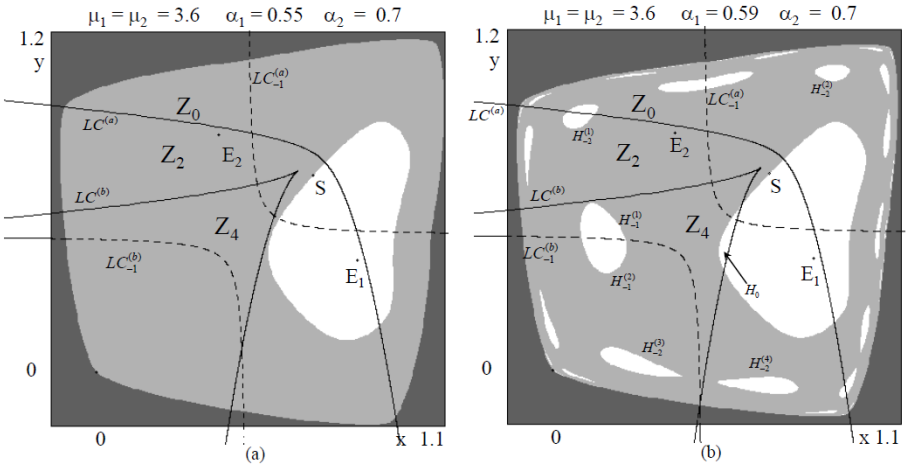

Figure 12.

[4]We follow the terminology introduced in [38].

So, as in the one-dimensional case, the global bifurcation which causes a transformation of a basin from connected set into the union of infinitely many non-connected portions, is caused by a contact between a critical set and a basin boundary. However, since the equations of the curves involved in the contact often cannot be analytically expressed in terms of elementary functions, the occurrence of contact bifurcations can only be revealed numerically. This happens frequently in the study of nonlinear dynamical systems of dimension greater than one: results on global bifurcations are generally obtained through an interplay between theoretical and numerical methods, and the occurrence of these bifurcations is shown by computer-assisted proofs, based on the knowledge of the properties of the critical curves and their graphical representation (see [40] for many examples). This "modus operandi" is typical in the study of global bifurcations of nonlinear two-dimensional maps.

3 Synchronization, riddling and intermittency phenomena

In this section we consider a two-dimensional dynamical system with an invariant unidimensional submanifold. For example, a dynamic game whose time evolution is represented by the iteration of a two-dimensional map in the case of identical players. This means that the dynamical system must remain the same if the variables x_1 and x_2 are interchanged, i.e. $T \circ P = P \circ T$, where $P : (x_1, x_2) \to (x_2, x_1)$ is the reflection through the diagonal Δ. This symmetry property implies that the diagonal is mapped into itself, i.e., $T(\Delta) \subseteq \Delta$, which corresponds with the obvious statement that, in a deterministic framework, identical players, starting from identical initial conditions, behave identically for each time. The trajectories embedded into Δ, i.e. characterized by $x_1(t) = x_2(t)$ for every t, are called *synchronized trajectories*, and they are governed by the one-dimensional map given by the restriction of T to the invariant submanifold Δ

$$\mathbf{x}_{t+1} = f(\mathbf{x}_t) \quad \text{with} \quad f = T|_{\Delta} : \Delta \to \Delta. \tag{15}$$

A trajectory starting out of Δ, i.e. with $x_0 \neq y_0$, is said to synchronize if $|x_1(t) - x_2(t)| \to 0$ as $t \to +\infty$. A question which naturally arises, in the case of symmetric competition models, is whether identical competitors starting from different initial conditions will synchronize, so that the asymptotic behavior is governed by the simpler one-dimensional model (15). This question can be reformulated as follows. Let A_s be an attractor of the one-dimensional map (15). Is it also an attractor for the two-dimensional map T? Of course, an attractor A_s of the restriction f is stable with respect to perturbations along Δ, so an answer to the question raised above can be given through a study of the stability of A_s with respect to perturbations transverse to Δ (*transverse stability*). If A_s is a cycle, then the study of the transverse stability is the usual one, based on the modulus of the eigenvalues of the cycle in the direction transverse to Δ, whereas the problem becomes more interesting when the dynamics restricted to the invariant submanifold are chaotic. Indeed, dynamical systems with chaotic trajectories embedded into an invariant submanifold of lower dimensionality than the total phase space have raised an increasing interest in the scientific community (see [5] and [23]), because the phenomenon of *chaos synchronization* may occur (see also [42]), i.e., the time evolution of the two competitors synchronize in the long run even if each of them behaves chaotically. Moreover, in this case, *Milnor attractors*, from [35], which are not stable in Lyapunov sense appear quite naturally in this context. To better understand the meaning of this point, we recall some definitions.

Definition 3.1. *A is an asymptotically stable attractor (or topological attractor) if it is Lyapunov stable, i.e. for every neighborhood U of A there exists a neighborhood V of A such that $T^t(V) \subset U$ for all $t \geq 0$, and $B(\mathcal{A})$ contains a neighborhood of A.*

In other words, If $\mathcal{A}$ is a topological attractor then a neighborhood $W \supset \mathcal{A}$ exists such that $T^t(\mathbf{x}) \to \mathcal{A}$ as $t \to +\infty$ for any $\mathbf{x} \in W$. In this case the stable set $\mathcal{B}(\mathcal{A})$, also called basin of attraction, is an open set given by $\mathcal{B}(\mathcal{A}) = \bigcup_{t \geq 0} T^{-t}(W)$.

Definition 3.2. *A closed invariant set A is said to be a weak attractor in Milnor sense (or simply Milnor attractor) if its stable set $B(\mathcal{A})$ has positive Lebesgue measure.*

Note that a topological attractor is also a Milnor attractor, whereas the converse is not true. Really the more general notion of Milnor attractor has been introduced to evidence the existence of invariant sets which "attract" many points even if they are not attractors in the usual topological sense.

We now recall some definitions and results related to the problem of chaos synchronization, see [23] for a more complete treatment. Let T be a map of the plane, Δ a one-dimensional trapping subspace and A_s a chaotic attractor (with absolutely continuous invariant measure on it) of the restriction (15) of T to Δ. The key property for the study of the transverse stability of A_s is that it includes infinitely many periodic orbits which are unstable in the direction along Δ. For any of these cycles it is easy to compute the associated eigenvalues. In fact, due to the symmetry of the map, the Jacobian matrix of T computed at any point of Δ, say $DT(x,x) = \{T_{ij}(x)\}$, is such that $T_{11} = T_{22}$ and $T_{12} = T_{21}$. The two orthogonal eigenvectors of such a symmetric matrix are one parallel to Δ, say $\mathbf{v}_{\|} = (1,1)$, and one perpendicular to it, say $\mathbf{v}_{\perp} = (1,-1)$, with related eigenvalues given by

$$\lambda_{\|}(x) = T_{11}(x) + T_{12}(x) \quad \text{and} \quad \lambda_{\perp}(x) = T_{11}(x) - T_{12}(x)$$

respectively. Of course, $\lambda_{\|}(x) = f'(x)$. Since the product of matrices with the structure of $DT(x,x)$ has the same structure as well, a k-cycle $\{s_1, ..., s_k\}$ embedded into Δ has eigenvalues $\lambda_{\|}^k = \prod_{i=1}^k \lambda_{\|}(s_i)$ and $\lambda_{\perp}^k = \prod_{i=1}^k \lambda_{\perp}(s_i)$, with eigenvectors $\mathbf{v}_{\|}$ and $\mathbf{v}_{\perp}$ respectively.

In the recent literature on chaos synchronization, stability statements are given in terms of the *transverse Lyapunov exponents*, by which the "average" local behavior of the trajectories in a neighborhood of the invariant set A_s can be understood, and new kinds of bifurcations can be detected , such as the *riddling bifurcation* or the *blowout bifurcation*. For a chaotic set $A_s \subset \Delta$, infinitely many transverse Lyapunov exponents can be defined as

$$\Lambda_{\perp} = \lim_{N \to \infty} \frac{1}{N} \sum_{i=0}^{N} \ln |\lambda_{\perp}(s_i)| \tag{16}$$

where $\{s_i = f^i(s_0), i \geq 0\}$ is a trajectory embedded in A_s.

If x_0 belongs to a k-cycle then $\Lambda_{\perp} = \ln |\lambda_{\perp}^k|$, so that the cycle is transversely stable if $\Lambda_{\perp} < 0$, whereas if x_0 belongs to a generic aperiodic trajectory embedded inside the chaotic set A_s then $\Lambda_{\perp}$ is the *natural transverse Lyapunov exponent* $\Lambda_{\perp}^{nat}$, where by the term "natural" we mean the Lyapunov exponent associated to the natural, or SBR (Sinai-Bowen-Ruelle), measure, i.e., computed for a typical trajectory taken in the chaotic attractor A_s. Since infinitely many cycles, all

unstable along Δ, are embedded inside a chaotic attractor A_s, a spectrum of transverse Lyapunov exponents can be defined, see [23],

$$\Lambda_\perp^{\min} \leq ... \leq \Lambda_\perp^{nat} \leq ... \leq \Lambda_\perp^{\max} \tag{17}$$

The meaning of the inequalities in (17) can be intuitively understood on the basis of the property that $\Lambda_\perp^{nat}$ expresses a sort of "weighted balance" between the transversely repelling and transversely attracting cycles (see [4], [34]). If $\Lambda_\perp^{\max} < 0$, i.e. all the cycles embedded in A_s are transversely stable, then A_s is asymptotically stable, in the usual Lyapunov sense, for the two-dimensional map T. However, it may occur that some cycles embedded in the chaotic set A_s become transversely unstable, i.e. $\Lambda_\perp^{\max} > 0$, while $\Lambda_\perp^{nat} < 0$. In this case, A_s is no longer Lyapunov stable, but it continues to be a *Milnor attractor,* i.e. it attracts a positive (Lebesgue) measure set of points of the two-dimensional phase space. So, if $\mathcal{A} \subset \Delta$ is a chaotic attractor of $T|_\Delta$ with absolutely continuous invariant measure, then a sufficient condition for a $\mathcal{A}$ be a Milnor, but not topological, attractor for the two-dimensional map T, is that

(a) at least one k-cycle embedded in $\mathcal{A}$ is transversely repelling, i.e. $\left|\lambda_\perp^{(k)}\right| > 1$, and

(b) the Lyapunov exponent $\Lambda_\perp^{nat}$ is negative.

This means that the majority of the trajectories on $\mathcal{A}$ are transversely attracting, but some (even infinitely many) trajectories inside $\mathcal{A}$ can exist whose transverse Lyapunov exponent is positive. In other words, transversely repelling trajectories can be embedded into a chaotic set which is attracting only "on average". In this case we have *weak stability* or *stability in Milnor sense*, but not asymptotic stability.

The transition from asymptotic stability to attractivity only in Milnor sense, marked by a change of sign of $\Lambda_\perp^{\max}$ from negative to positive, is denoted as the *riddling bifurcation* in [32] (or *bubbling bifurcation* in [44]). Even if the occurrence of such bifurcations is detected through the study of the transverse Lyapunov exponents, their effects depend on the action of the non linearities far from Δ, that is, on the global properties of the dynamical system. In fact, after the riddling bifurcation two possible scenarios can be observed according to the fate of the trajectories that are locally repelled along (or near) the local unstable manifolds of the transversely repelling cycles:

(L): they can be reinjected towards Δ, so that the dynamics of such trajectories are characterized by some bursts far from Δ before synchronizing on it (a very long sequence of such bursts, which can be observed when $\Lambda_\perp$ is close to zero, has been called *on-off intermittency* in [41]);

(G): they may belong to the basin of another attractor, in which case the phenomenon of *riddled basins* ([4]) is obtained.

Some authors call *local riddling* the situation (L) and, by contrast, *global riddling* the situation (G) (see [5, 34] and [33]). When also $\Lambda_\perp^{nat}$ becomes positive, due to the fact that the transversely unstable periodic orbits embedded into A_s have a greater weight as compared with the stable ones, a *blowout bifurcation* occurs, after which A_s is no longer a Milnor attractor, because it attracts a set of points of zero measure, and becomes a *chaotic saddle*, see [23]. In particular, for $\lambda_\perp^{\min} > 0$ all the cycles embedded into Δ are transversely repelling, and A_s is called *normally repelling chaotic saddle*. Also the macroscopic effect of a blowout bifurcation is strongly influenced by the behavior of the dynamical system far from the invariant submanifold Δ: The trajectories starting close to the chaotic saddle may be attracted by some attracting set far from Δ or remain inside a two-dimensional compact set located around the chaotic saddle A_s, thus giving on-off intermittency.

As noticed by many authors, (see [5, 23] and [34]), even if the occurrence of riddling and blowout bifurcations is detected through the transverse Lyapunov exponents, i.e. from a local

analysis of the linear approximation of the map near Δ, their effects are determined by the global properties of the map. In fact, the effect of these bifurcations is related to the fate of the trajectories which are locally repelled away from a neighborhood of the Milnor attractor A_s, since they may reach another attractor or they may be folded back toward A_s by the action of the nonlinearities acting far from Δ. When T is a noninvertible map, as generally occurs in problems of chaos synchronization[5], the global dynamical properties can be usefully described by the method of *critical curves* and the reinjection of the locally repelled trajectories can be described in terms of their folding action.

This idea has been recently proposed in [21], for the study of symmetric maps arising in game theory, where the critical curves have been used to obtain the boundary of a compact *absorbing area* inside which intermittency and blowout phenomena are confined. In other words, the critical curves are used to bound a compact region of the phase plane that acts as a trapping bounded vessel inside which the trajectories starting near S are confined. In particular, in [10], the concept of *minimal invariant absorbing area* is used in order to give a global characterization of the different dynamical scenarios related to riddling and blowout bifurcations. In order to give an example, let us consider the map

$$T_s : \begin{cases} x' = \mu y(1-y) + \varepsilon(y-x) \\ y' = \mu x(1-x) + \varepsilon(x-y) \end{cases} \tag{18}$$

The restriction $T_s|_\Delta$ to the invariant diagonal Δ can be identified with the one-dimensional logistic map

$$x' = f_\mu(x) = \mu x(1-x). \tag{19}$$

The eigenvalues of the symmetric Jacobian matrix $DT(x,x)$ are

$$\rho_\parallel(x) = \mu - 2\mu x \quad , \quad \rho_\perp(x) = 2\mu x - \mu - 2\varepsilon.$$

with eigenvectors which are parallel to Δ ($\mathbf{v}_\parallel = (1,1)$) and orthogonal to Δ ($\mathbf{v}_\perp = (1,-1)$) respectively. It is important to note that the coupling parameter ε only appears in the transverse eigenvalue $\lambda_\perp$, i.e. ε is a *normal parameter*: it has no influence on the dynamics along the invariant submanifold Δ, and only influences the transverse stability. This allows us to consider fixed values of the parameter μ, such that a chaotic attractor $A_s \subset \Delta$ of the map (19) exists, with an absolutely continuous invariant measure on it. So, we can study the transverse stability of A_s as the coupling between the two components, measured by the parameter ε, varies. Suitable values of the parameter μ, at which chaotic intervals for the restriction (19) exist, are obtained from the well known properties of the logistic map (see [36]). For example, at the parameter value $\overline{\mu}_2 = 3.5748049387592...$ the period-4 cycle of the logistic map undergoes the homoclinic bifurcation, at which four cyclic chaotic intervals are obtained by the merging of 8 cyclic chaotic intervals. By using $\overline{\mu}_2$ we get a four-band chaotic set A_s along the diagonal Δ, as shown in Figure 13a. In this case, for $\varepsilon = 0.24$ we have $\Lambda_\perp^{\max} > 0$ and $\Lambda_\perp^{nat} = -4.7 \times 10^{-3} < 0$. Hence, A_s is a Milnor attractor and local riddling occurs. The generic trajectory starting from initial conditions taken in the white region of Figure 13a leads to asymptotic synchronization. In Figure 13a the asymptotic part of a trajectory is shown, after a transient of $15,000$ iterations has been discarded.

[5]In fact the one-dimensional restriction f must be a noninvertible map in order to have chaotic motion along the invariant subspace Δ.

Indeed, if also the transient is represented, Figure 13b is obtained. During the transient, the time evolution of the system is characterized by several bursts away from Δ before synchronization occurs, as shown in Figure 14, where the difference $x_t - y_t$, computed along the trajectory of Figure 13, is represented versus time. It it worth to note the intermittent behavior of the trajectory: sometimes it seems to synchronize for a quite long number of iterations, then a sudden burst occurs. This phenomenon is also called *on-off intermittency.*

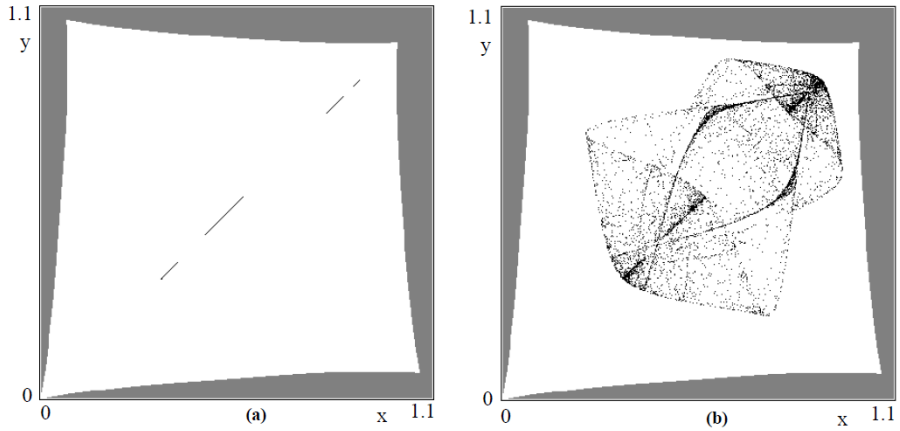

Figure 13.

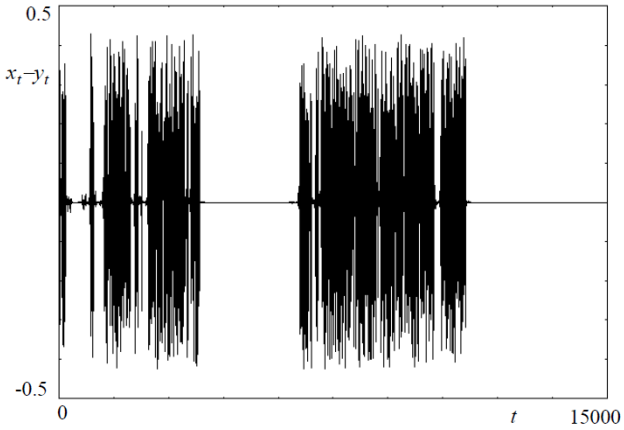

Figure 14.

The Milnor attractor A_s is included inside a minimal invariant absorbing area whose boundary can be easily obtained by five iterations of an arc of LC_{-1}, as shown in Figure 21a. This absorbing area, obtained by the procedure outlined in section 3, constitutes a trapping region inside which the bursts observed during the transient are contained. This means that, even if it is difficult to predict the sequence of times at which asynchronous bursts occur, an estimate of their maximum amplitude can be obtained by the construction of the minimal invariant absorbing area which includes the Milnor attractor on which synchronized dynamics take place. In such a situation, a method to obtain a trajectories which never synchronize, so that the bursts never stop and the iterated points fill up the whole minimal absorbing area, consists in the introduction of a small parameters' mismatch, such as ε_1 slightly different from ε_2 or μ_1 slightly different from μ_2, so

that the symmetry is broken (see [10] and [11] for example). This implies that the invariance of Δ is lost, and consequently the one-dimensional Milnor attractor embedded in no longer exists.

A similar effect is obtained even in the symmetric case, if the value of the coupling parameter ε is increased so that $\Lambda_{\perp}^{nat}$ increases until it becomes positive, i.e. a blowout bifurcation occurs. After this bifurcation the bursts which characterize the first part of the trajectory of Figures 13 and 14, never stop, i.e. the firms never synchronize. A_s is now a chaotic saddle, and on-off intermittency is observed. This is what happens in the situation shown in Figure 15b, obtained for $\varepsilon = 0.245$, at which $\Lambda_{\perp}^{nat} = 2.2 \times 10^{-2} > 0$. Now the point of a generic trajectory starting from the white region fill the whole absorbing area, still bounded by segments of critical arcs.

We end this short survey by stressing that if the absorbing area bounded by segments of critical curves, inside which riddling phenomena and on-off intermittency occurs, has a contact with the boundary of the basin around it, then the phenomenon of riddles basins suddenly appears, see [11] for an example.

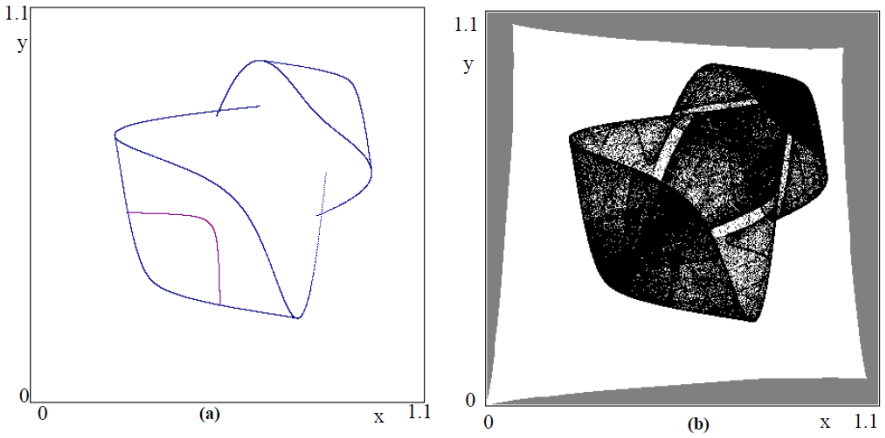

Figure 15.

4 Maps with Vanishing Denominators

Let us consider a two-dimensional discrete dynamical system defined by

$$(x_{t+1}, y_{t+1}) = T\,(x_t, y_t) = (F(x_t, y_t), G(x_t, y_t))\,,$$

where at least one of the components F or G has a denominator which can vanish in a one-dimensional subset of the phase plane. This implies that the iterated map T is not defined in the whole plane, and this causes the occurrence of some particular dynamic behaviors and global bifurcations that cause qualitative changes in the topological structure of the attractors and the basins of attraction. In [13, 15] and [16] these dynamic phenomena have been associated with the existence of points where one of the components of the map T or some of its inverse(s) T^{-1} assumes the form $0/0$. In these papers the concepts of *focal point* and *prefocal curve* have been introduced, and several kinds of global bifurcations have been described that lead to the creation of particular structures of the basins of attraction called *lobes* and *crescents*, characterized by fan-shaped boundaries issuing from the focal points, where one component of T becomes $0/0$ (see points denoted by Q in Figure 16, taken from [13, 20] and [25] respectively). Roughly speaking,

a *prefocal curve* is a set of points for which at least one inverse exists which maps (or "focalizes") the whole set into a single point, called *focal point*.

The global bifurcations that cause the creation of structures of the basins which are peculiar of maps with a vanishing denominator have been explained in [13] and [15] in terms of contacts between basin boundaries and prefocal curves. These definitions and properties have been studied by considering the image of an arc crossing through a simple focal point (i.e. located at a transverse intersection of the curve of vanishing denominator and that of vanishing numerator) and a one-to-one correspondence is obtained between the slopes of the arcs through a focal point and the points in which their images cross the corresponding prefocal set. This implies that the preimages of any curve crossing the prefocal set in two points includes a loop with a knot in the focal point, and this is the basic mechanism leading to the formation of *lobes* and *crescents*

These singularities may also be important in the study of maps defined in the whole plane, but such that some of the inverses have a vanishing denominator and possess focal points. These dynamic phenomena have been observed in several dynamic models used ti describe real world systems, for example in dynamic economic models (such as the basins shown in Figure 16a, from [20]), or in iterative numeric methods coming from the application of Newton's or Bairstow's method for finding the zeroes of functions (see the basins shown in Figure 16c, from [25]). The structure of the basins in Figure 16 clearly shows the presence of focal points, from which fans of different colors spread.

These concepts, proposed in the framework of the theory of iteration of two-dimensional real maps, using the style and terminology of the theory of dynamical systems, can be compared with the concepts of *exceptional locus* and *blow-up* in the framework of the study of rational maps in the literature on algebraic geometry.

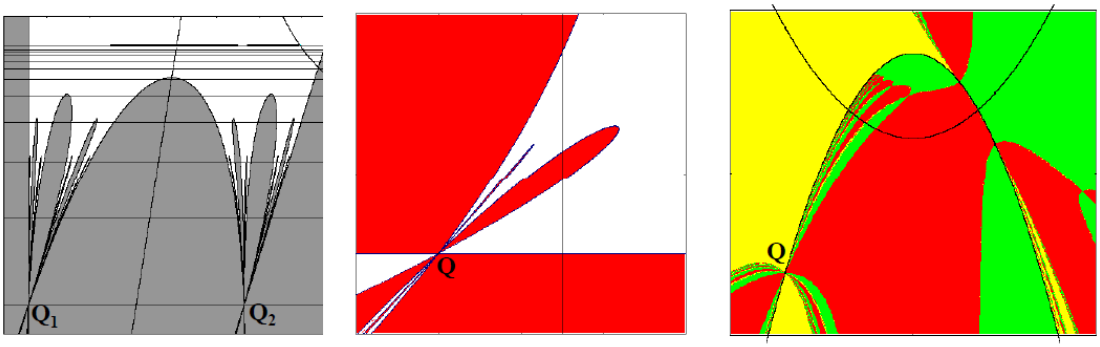

(a) (b) (c)

Figure 16.

4.1 Definitions and basic properties

In order to simplify the exposition, we assume that only one of the two functions defining the map T has a denominator which can vanish, say

$$T : \begin{cases} x' = F(x,y) \\ y' = G(x,y) = N(x,y)/D(x,y) \end{cases}$$

where x and y are real variables, $F(x,y)$, $N(x,y)$ and $D(x,y)$ are continuously differentiable functions (N and D without common factors) and defined in the whole plane $\mathbb{R}^2$. The *set of*

nondefinition of the map T (given by the set of points where at least one denominator vanishes) reduces to

$$\delta_s = \{(x, y) \in \mathbb{R}^2 | D(x, y) = 0\}.$$

Let us assume that δ_s is given by the union of smooth curves of the plane. The two-dimensional recurrence obtained by the iteration of T is well defined provided that the initial condition belongs to the set E given by $E = \mathbb{R}^2 \setminus \bigcup_{k=0}^{\infty} T^{-k}(\delta_s)$, where $T^{-k}(\delta_s)$ denotes the set of the rank-k preimages of δ_s, i.e. the set of points which are mapped into δ_s after k applications of T ($T^0(\delta_s) \equiv \delta_s$). Indeed, in order to generate non interrupted sequences by the iteration of the map T, the points of δ_s, as well as all their preimages of any rank, constitute a set of zero Lebesgue measure which must be excluded from the set of initial conditions so that $T : E \to E$.

Let us consider a bounded and smooth simple arc γ, parametrized as $\gamma(\tau)$, transverse to δ_s, such that $\gamma \cap \delta_s = \{(x_0, y_0)\}$ and $\gamma(0) = (x_0, y_0)$. We are interested in its image $T(\gamma)$. As $(x_0, y_0) \in \delta_s$ we have, according to the definition of δ_s, $D(x_0, y_0) = 0$. If $N(x_0, y_0) \neq 0$, then $\lim_{\tau \to 0\pm} T(\gamma(\tau)) = (F(x_0, y_0), \infty)$ where ∞ means either $+\infty$ or $-\infty$. This means that the image $T(\gamma)$ is made up of two disjoint unbounded arcs asymptotic to the line of equation $x = F(x_0, y_0)$. A different situation may occur if the point (x_0,y_0) $\in \delta_s$ is such that not only the denominator but also the numerator vanishes in it, i.e. $D(x_0, y_0) = N(x_0, y_0) = 0$. In this case the second component of T assumes the form 0/0. This implies that the limit above may give rise to a finite value, so that the image $T(\gamma)$ is a bounded arc (see Figure 2a) crossing the line $x = F(x_0, y_0)$ in the point $(F(x_0, y_0), y)$, where

$$y = \lim_{\tau \to 0} G(x(\tau), y(\tau)).$$

It is clear that the limiting value y must depend on the arc γ. Furthermore it may have a finite value along some arcs and be infinite along other ones. This leads to the following definition of *focal point* and *prefocal curve* [13]:

Definition 4.1. *Consider the map T (x,y)*$\to (F(x, y), N(x, y)/D(x, y))$. *A point Q=(*$x_0$,$y_0$*) is a focal point of T if* $D(x_0, y_0) = N(x_0, y_0) = 0$ *and there exist smooth simple arcs* $\gamma(\tau)$*, with* $\gamma(0)$*=Q, such that* $\lim_{\tau \to 0} T(\gamma(\tau))$ *is finite. The set of all such finite values, obtained by taking different arcs* $\gamma(\tau)$ *through Q, is the prefocal set* δ_Q*, the equation of which is* $x = F(Q)$.

Here we shall only consider *simple focal points*, i.e. points which are simple roots of the algebraic system $N(x, y) = 0$, $D(x, y) = 0$. Thus a focal point $Q = (x_0, y_0)$ is simple if $\overline{N}_x \overline{D}_y - \overline{N}_y \overline{D}_x \neq 0$, where $\overline{N}_x = \frac{\partial N}{\partial x}(x_0, y_0)$ and analogously for the other partial derivatives. In this case (of a simple focal point) there exists a one-to-one correspondence between the point $(F(Q), y)$, in which $T(\gamma)$ crosses δ_Q, and the slope m of $\overline{\gamma}$ in Q (as shown in [13]):

$$m \to (F(Q), y(m)), \text{ with } y(m) = (\overline{N_x} + m\overline{N_y}) \,/\, (\overline{D_x} + m\overline{D_y}),$$

and

$$(F(Q), y) \to m(y), \text{ with } m(y) = (\overline{D_x} y - \overline{N_x}) \,/\, (\overline{N_y} - \overline{D_y} y).$$

From the definition of the prefocal curve, it follows that the Jacobian $\det\left(DT^{-1}\right)$ must necessarily vanish in the points of δ_Q. Indeed, if the map T^{-1} is defined in δ_Q, then all the points

of the line δ_Q are mapped by T^{-1} into the focal point Q. This means that T^{-1} is not locally invertible in the points of δ_Q, being it a many-to-one map, and this implies that its Jacobian cannot be different from zero in the points of δ_Q. From the relations given above it results that different arcs γ_j, passing through a focal point Q with different slopes m_j, are mapped by T into bounded arcs $T(\gamma_j)$ crossing δ_Q in different points $(F(Q), y(m_j))$ (figs. 17b,c). Interesting properties are obtained if the inverse of T (or the inverses, if T is a noninvertible map) is (are) applied to a curve that crosses a prefocal curve.

Nonsimple focal points are considered in [16], where it is shown that they are generally associated with particular bifurcations.

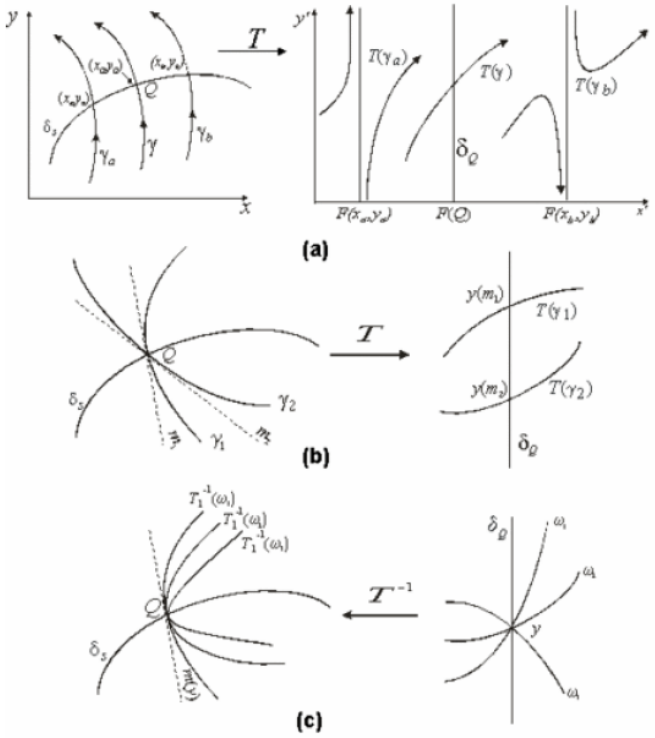

Figure 17.

4.2 Case of an invertible map

Let T be invertible, and δ_Q a prefocal curve whose corresponding focal point is Q (and several prefocal curves may exist, each having a corresponding focal point). Then each point sufficiently close to δ_Q has its rank-1 preimage in a neighborhood of the focal point Q. If the inverse T^{-1} is continuous along δ_Q then all the points of δ_Q are mapped by T^{-1} in the focal point Q. Roughly speaking we can say that the prefocal curve δ_Q is "*focalized*" by T^{-1} in the focal point Q, i.e. $T^{-1}(\delta_Q) = Q$. We note that the map T is not defined in Q, thus T^{-1} cannot to be strictly considered as an inverse of T in the points of δ_Q, even if T^{-1} is defined in δ_Q.

The relation given above implies that the preimages of different arcs crossing the prefocal curve δ_Q in the same point $(F(Q), y)$ are given by arcs all crossing the singular set through Q, and all with the same slope $m(y)$ in Q. Indeed, consider different arcs ω_n, crossing δ_Q in the same point $(F(Q), y)$ with different slopes, then these arcs are mapped by the inverse T^{-1} into different

arcs $T^{-1}(\omega_n)$ through Q, all with the same tangent, of slope $m(y)$, according to the formula given above. They must differ by the curvature at the point Q.

4.3 Case of a non invertible map

4.3.1 General considerations

In the case of a continuous noninvertible map T, several focal points may be associated with a given prefocal curve δ_Q, each with its own one-to-one correspondence between slopes and points. The phase space of a *noninvertible map* is subdivided into open regions (or zones) Z_k, whose points have k distinct rank-1 preimages, obtained by the application of k distinct inverse maps T_j^{-1} (i.e. such that $T_j^{-1}(x,y) = (x_j, y_j)$, $j = 1, ..., k$).

From the properties of maps with a vanishing denominator it results that generally a focal point Q belongs to the set $\overline{LC_{-1}} \cap \delta_S$, where $\overline{LC_{-1}}$ denotes the closure of LC_{-1}, but in particular bifurcation cases, in which δ_S belongs to J_C, it happens that a focal point Q may not belong to $\overline{LC_{-1}}$. The geometric behavior and the plane's foliation are different in the two cases. This leads to two different situations, according to the fact that the focal points belong or not to the set $\overline{LC_{-1}}$.

4.3.2 The focal points do not belong to $\overline{\mathbf{LC_{-1}}}$.

The following properties have been shown in [13]. (a) *For each prefocal curve δ_Q we have $LC \cap \delta_Q = \emptyset$.* (b) *If all the inverses are continuous along a prefocal curve δ_Q, then the whole prefocal set δ_Q belongs to a unique region Z_k in which k inverse maps T_j^{-1} , j=1,...,k, are defined.*

It is plain that for a prefocal δ_Q at least one inverse is defined that "focalizes" it into a focal point Q. However, other inverses may exist that "focalize" it into distinct focal points, all associated with the same prefocal curve δ_Q. These focal points are denoted as $Q_j = T_j^{-1}(\delta_Q)$, $j = 1, ..., n$, with $n \leq k$. For each focal point Q_j the same results given above can be obtained with T^{-1} replaced by T_j^{-1}, so that for each Q_j a one-to-one correspondence $m_j(y)$ in the form given above is defined. With similar arguments it is easy to see that an arc ω crossing δ_Q in a point $(F(Q), y)$, where $F(Q) = F(Q_j)$ for any j, is mapped by each T_j^{-1} into an arc $T_j^{-1}(\omega)$, through the corresponding Q_j with the slope $m_j(y)$. If different arcs are considered, crossing δ_Q in the same point, then these are mapped by each inverse T_j^{-1} into different arcs through Q_j, all with the same tangent. We note that property (a) given above implies that the critical curve LC is generally asymptotic to the prefocal curves (several examples are shown in [13]).

4.3.3 The focal points belong to $\overline{\mathbf{LC_{-1}}}$.

When the focal points belong to $\overline{LC_{-1}}$ (closure of LC_{-1}) the "geometrical" situations of the phase plane, and the bifurcation types, are more complex (see [15]) with respect to the previous case. This is due to the fact that now LC has contact points at finite distance with the prefocal curves. The property $Q_j = T_j^{-1}(\delta_Q)$, $j = 1, \ldots, n$, with $n \leq k$, does not occur. Now in the generic case a given prefocal curve δ_Q is not associated with several focal points Q_j. Only one of the inverses T_j^{-1} maps a non critical point of a given prefocal curve into its related focal point, so that we can write $Q = T_j^{-1}(F(Q), y)$ (or $Q = T_j^{-1}(\delta_Q)$ for short), but the index j depends on the non critical point $(F(Q), y)$ considered on δ_Q. For this reason the previous situation of δ_Q (focal points do not belong to $\overline{LC_{-1}}$) appears as non generic (indeed it may result from the merging of two prefocal curves δ_Q^r and δ_Q^s without merging of the corresponding focal points, as shown in [15]).

A qualitative illustration is given in Figure 18, where a situation with two prefocal curves is represented for a noninvertible map T, $(x, y) \to (x', y')$, of type $(Z_0\text{-}Z_2)$. The inverse relation $T^{-1}(x', y')$ has two components in the region Z_2, denoted by T_1^{-1} and T_2^{-1}, and no real components in the region Z_0. The set of nondefinition δ_s is a simple straight line, and there are two prefocal lines, δ_{Q_i}, of equation $x = F(Q_i)$, associated with the focal points Q_i, $i = 1, 2$, respectively, and $V_i = LC \cap \delta_{Q_i}$ are the points of tangency between LC and the two prefocal curves. Let δ'_{Q_i} be the segment of δ_{Q_i} such that $y < y(V_i)$ (continuous line in Figure 18), and δ''_{Q_i} the segment of δ_{Q_i} such that $y > y(V_i)$ (segmented line in Figure 18). The "focalization" occurs in the following way:

$$T_1^{-1}(\delta'_{Q_i}) = Q_i, \qquad T_2^{-1}(\delta''_{Q_i}) = Q_i$$

with $T_2^{-1}(\delta'_{Q_i}) \cup T_1^{-1}(\delta''_{Q_i}) = \pi_i$, $i = 1, 2$, being the two lines passing through the focal points Q_i and tangent to LC_{-1}at these points. When $\delta_{Q_1} \to \delta_{Q_2}$, due to a parameter variation, without merging of the focal points, the points V_i on the prefocal curves tend to infinity, i.e. $\delta_{Q_1} = \delta_{Q_2}$ becomes an asymptote for LC.

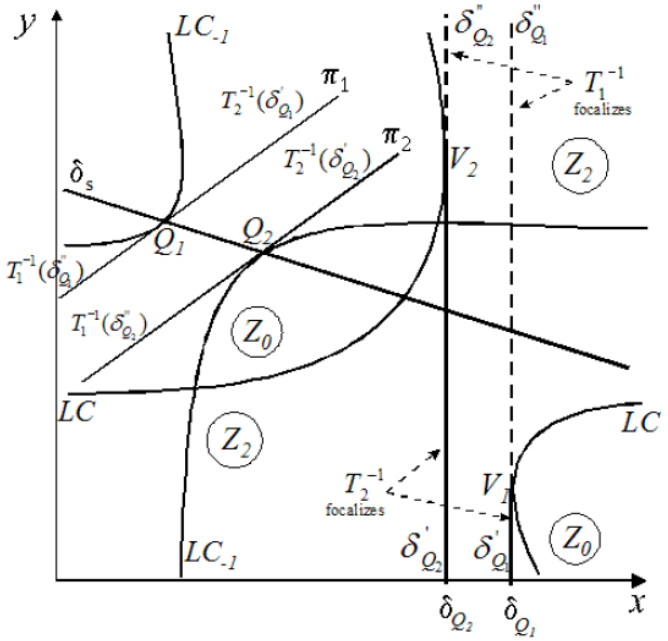

Figure 18.

These situations can be easily observed, for example, by using the following map T_e (see [13])

$$T_e : \begin{cases} x' = y + \varepsilon x \\ y' = \frac{\alpha x^2 + \gamma x}{y - \beta + \sigma x} \end{cases}$$

not defined in the points of the line δ_s of equation $y - \beta + \sigma x = 0$, on which two focal points exist given by $Q_1 = (0,\ \beta)$, $Q_2 = (-\frac{\gamma}{\alpha},\ \beta + \frac{\gamma\delta}{\alpha})$ and the corresponding prefocal curves δ_{Q_i}, of equation $x = F(Q_i)$, $i = 1, 2$, are $x = \beta$ and $x = \beta - (\varepsilon - \sigma)\,\gamma/\alpha$ respectively.

The map T_e is a noninvertible map of $(Z_0$-$Z_2)$ type with inverses defined by

$$T_{e1,e2}^{-1}: \begin{cases} x = \frac{1}{2\alpha}\left((\sigma-\varepsilon)\,y' - \gamma\right) \mp \sqrt{\Delta\,(x',y')} \\ y = x' - \varepsilon x \end{cases}$$

where $\Delta(x',y') = (\gamma - \sigma y' + \varepsilon y')^2 - 4\alpha\,(\beta y' - x'y') > 0$ in the region Z_2 and $LC = \{(x,y)\,|\,\Delta(x',y') = 0\}$. In Figure 19a, obtained with parameters $\alpha = 0.5$, $\gamma = 0.5$, $\beta = \sqrt{2}$, $\sigma = 0.2$, $\varepsilon = -0.2$, a situation similar to the one shown in Figure 1 is obtained (the colored region represents the basin of the stable fixed point $O = (0,0)$ and the complementary region the basin of infinity). In Figure 19b, obtained with $\varepsilon = \sigma = 0.1$ and the other parameters unchanged, the two focal points are still distinct, but the two prefocal lines merge and become an asymptote for LC. Note that we have $LC_{-1} = J_C = J_0$ before the bifurcation, while at the bifurcation the hyperbola LC_{-1} degenerates into two lines, the vertical branch gives the new critical set LC_{-1} and the other collapses into the singular set δ_s. At this bifurcation $LC_{-1} = J_0 \subset J_C$ (because J_C also includes the set of nondefinition δ_s), the resulting "double" prefocal curve is an asymptote of LC, the arcs π_1 and π_2 degenerate into the focal points, which now are not located on $\overline{LC_{-1}}$.

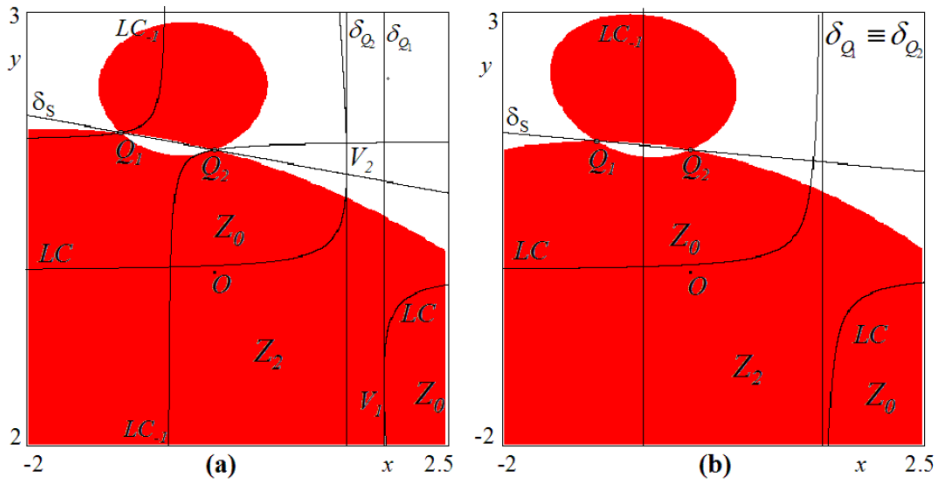

Figure 19.

4.4 Some dynamic properties of focal points

Important effects on the geometric and dynamical properties of the map T can be observed, due to the existence of a vanishing denominator. Indeed, a contact between a curve segment γ and the singular set δ_s causes noticeable qualitative changes in the shape of the image $T(\gamma)$. Moreover, a contact of an arc ω with a prefocal curve δ_Q, gives rise to important qualitative changes in the shape of the preimages $T_j^{-1}(\omega)$. When the arcs ω are portions of phase curves of the map T, such as *invariant closed curves*, *stable or unstable sets* of saddles, *basin boundaries*, we have that contacts between singularities of different nature generally induce important qualitative changes, which constitute *new types of global bifurcations* that change the structure of the attracting sets, or of their basins.

In order to simplify the description of geometric and dynamic properties of maps with a vanishing denominator, and their particular global bifurcations, we assume that δ_s and δ_Q are made up of branches of simple curves of the plane. Let us describe what happens to the images of a small

curve segment γ when it has a tangential contact with δ_s and then crosses it in two points, and what happens to the preimages of a small curve segment ω when it has a contact with a prefocal curve δ_Q and then crosses it in two points.

4.4.1 Action of the map

Consider first a bounded curve segment γ that lies entirely in a region in which no denominator of the map T vanishes, so that the map is continuous in all the points of γ. As the arc γ is a compact subset of $\mathbb{R}^2$, also its image $T(\gamma)$ is compact (see the upper qualitative sketch in Figure 20). Suppose now to move γ towards δ_s, until it becomes tangent to it in a point $A_0 = (x_0, y_0)$ which is not a focal point. This implies that the image $T(\gamma)$ is given by the union of two disjoint and unbounded branches, both asymptotic to the line σ of equation $x = F(x_0, y_0)$. Indeed, $T(\gamma) = T(\gamma_a) \cup T(\gamma_b)$, where γ_a and γ_b are the two arcs of γ separated by the point $A_0 = \gamma \cap \delta_s$. The map T is not defined in A_0 and the limit of $T(x, y)$ assumes the form $(F(x_0, y_0), \infty)$ as $(x, y) \to A_0$ along γ_a, as well as along γ_b. In such a situation any image of γ of rank $k > 1$, given by $T^k(\gamma)$, includes two disjoint unbounded branches, asymptotic to the rank-k image of the line σ, $T^k(\sigma)$. When γ crosses through δ_s in two points, say $A_1 = (x_1, y_1)$ and $A_2 = (x_2, y_2)$, both different from focal points, then the asymptote σ splits into two disjoint asymptotes σ_1 and σ_2 of equations $x = F(x_1, y_1)$ and $x = F(x_2, y_2)$ respectively, and the image $T(\gamma)$ is given by the union of three disjoint unbounded branches (see the lower sketch in Figure 20).

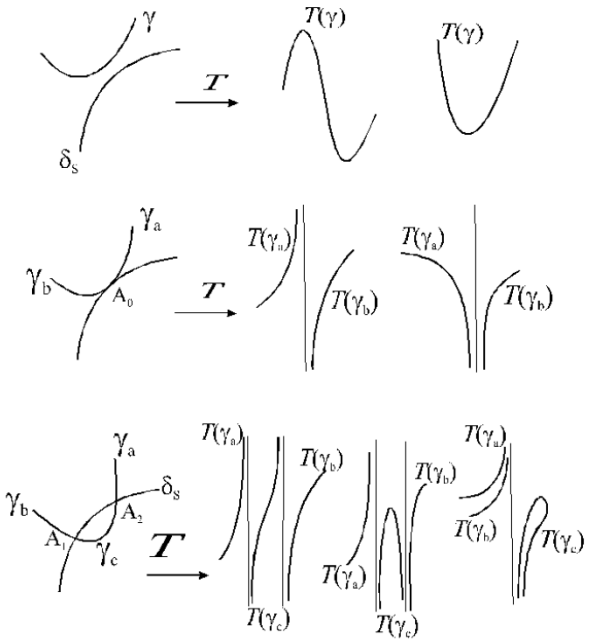

Figure 20.

When γ is, for example, the local unstable manifold W^u of a saddle point or saddle cycle, the qualitative change of $T(\gamma)$, due to a contact between γ and δ_s, as described above, may represent an important contact bifurcation of the map T. Indeed the creation of a new unbounded branch of W^u, due to a contact with δ_s, may cause the *creation of homoclinic points*, from new transverse intersections between the stable and unstable sets, W^s and W^u, of the same saddle point (or cycle).

In such a case it is worth noting that the corresponding *homoclinic bifurcation* does not come from a tangential contact between W^u and W^s. For maps with a vanishing denominator, this implies that homoclinic points can be created without a homoclinic tangency between W^u and W^s, from the sudden creation of unbounded branches of W^u when it crosses through δ_s (see [13]). If before the bifurcation W^u is associated with a chaotic attractor, the *homoclinic bifurcation* resulting from the contact between W^u and δ_s may gives rise to an *unbounded chaotic attractive set made up of unbounded, but not diverging, chaotic trajectories* (see [14]). If before the bifurcation W^u is not associated with a chaotic attractor, the *homoclinic bifurcation* resulting from the contact between W^u and δ_s may gives rise to a *basin explosion* as described in [13]

If the map is noninvertible, a direct consequence of the above arguments concerns the action of the curve of nondefinition δ_s on LC_{-1}. *If* $\overline{LC_{-1}}$ *has* n *transverse intersections with the set* δ_s *in non focal points* $P_i = (x_i, y_i)$, $i = 1, .., n$, *then the critical set* $LC = T(LC_{-1})$ *includes* $(n+1)$ *disjoint unbounded branches, separated by the n asymptotes* σ_i *of equation* $x = F(x_i, y_i)$, $i = 1, .., n$.

4.4.2 Action of the inverses

(a) Let T be an *invertible map,* $T(x, y) = (F(x, y), N(x, y)/D(x, y)$. Consider a smooth curve segment ω that moves towards a prefocal curve δ_Q until it crosses through δ_Q (see Figure 21) so that only a focal point $Q = T^{-1}(\delta_Q)$ is associated with δ_Q. The prefocal set δ_Q belongs to the line of equation $x = F(Q)$, and the one-to-one correspondences between slopes and points hold. When ω moves toward δ_Q, its preimage $\omega_{-1} = T^{-1}(\omega)$ moves towards Q. If ω becomes tangent to δ_Q in a point $C = (F(Q), y_c)$, then ω_{-1} has a cusp point at Q. The slope of the common tangent to the two arcs, that join at Q, is given by $m(y_c)$. If the curve segment ω moves further, so that it crosses δ_Q at two points $(F(Q), y_1)$ and $(F(Q), y_2)$, then ω_{-1} forms a *loop with a double point* at the focal point Q. Indeed, the two portions of ω that intersect δ_Q are both mapped by T^{-1} into arcs through Q, and the tangents to these two arcs of ω_{-1}, issuing from the focal point, have different slopes, $m(y_1)$ and $m(y_2)$ respectively, according to the formulas given above.

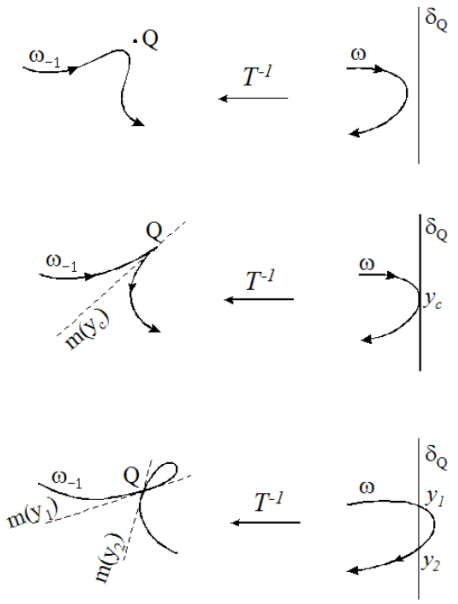

Figure 21.

(b) Now let T be a *noninvertible map with focal points not located on* $\overline{LC_{-1}}$. In this case $k \geq 1$ distinct focal points Q_j, $j = 1, ..., k$, may be associated with a prefocal curve δ_Q. Then each inverse T_j^{-1}, $j = 1, ..., k$, gives a distinct preimage $\omega_{-1}^j = T_j^{-1}(\omega)$ which has a cusp point in Q_j, $j = 1, ..., k$, when the arc ω is tangent to δ_Q. Each preimage ω_{-1}^j gives rise to a loop in Q_j when the arc ω intersects δ_Q in two points (see Figure 22, concerning the case $k = 2$).

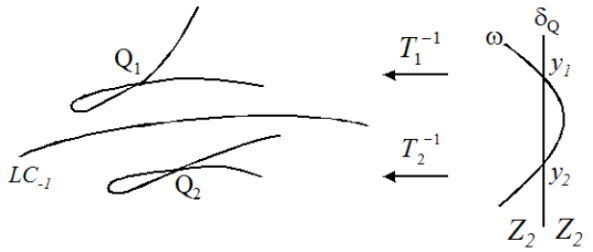

Figure 22.

When ω is an arc belonging to a basin boundary $\mathcal{F}$, the qualitative modifications of the preimages $T_j^{-1}(\omega)$ of ω, due to a tangential contact of ω with the prefocal curve, can be particularly important for the global dynamical properties of the map T. As a frontier $\mathcal{F}$ generally is backward invariant, i.e. $T^{-1}(\mathcal{F}) = \mathcal{F}$, if ω is an arc belonging to $\mathcal{F}$, then all its preimages of any rank must belong to $\mathcal{F}$. This implies that if a portion ω of $\mathcal{F}$ has a tangential contact with a prefocal curve δ_Q, then necessarily at least k cusp points, located in the focal points Q_j, are included in the boundary $\mathcal{F}$. Moreover, if the focal points Q_j have preimages, then also they belong to $\mathcal{F}$, so that further cusps exist on $\mathcal{F}$, with tips at each of such preimages. It results that if the basin boundary $\mathcal{F}$ was smooth before the contact with the prefocal curve δ_Q, such a contact gives rise to points of non smoothness, which may be infinitely many if some focal point Q_j has preimages of any rank, with possibility of fractalization of $\mathcal{F}$ when it is nowhere smooth. When $\mathcal{F}$ crosses through δ_Q in two points, after the contact $\mathcal{F}$ must contain at least k loops with double points in Q_j. Also in this case, if some focal point Q_j has preimages, other loops appear (even infinitely many, with possibility of fractalization) with double points in the preimages of any rank of Q_j, $j = 1, ..., n$.

(c) Whatever be the map T (invertible, or not, with focal points on $\overline{LC_{-1}}$ or not) *a contact of a basin boundary with a prefocal curve gives rise to a new type of basin bifurcation that causes the creation of cusp points and, after the crossing, of loops (called "lobes"), along the basin boundary*. This may give rise to a very particular fractalization of the basin boundary ([9, 13]).

(d) Let T be a *noninvertible map with focal points not located on* $\overline{LC_{-1}}$. In this case the contact of two *lobes* on LC_{-1} (related to a contact of LC with the basin boundary) gives rise to a *crescent* bounded by the two focal points, from which lobes appeared. *The creation of "crescents" [13], resulting from the contact of lobes, is specific to noninvertible maps with denominator,when the focal points are not located on* $\overline{LC_{-1}}$. It requires the intersection of the boundary with a prefocal curve (located in a region with more than one inverse), at which the lobes are created, followed by a contact with a critical curve, causing the contact and merging of the lobes. At the contact the lobes are not tangent to LC_{-1}. After the contact, they merge creating the crescent.

(e) If T is a *noninvertible map with focal points located on* $\overline{LC_{-1}}$, then in the generic case we have a behavior similar to that of the invertible case, in which only one focal point is associated with δ_Q, but in a more complex situation with respect to the role of the components of the inverse

map on δ_Q, and the presence of the arcs denoted δ'_{Q_i} and δ''_{Q_i} in Figure 18. Details on this situation are given in [15]. Now a *crescent* does not results from the contact of two lobes, but from *the contact of a lobe (issuing from a focal point) with another focal point*. This situation is specific to noninvertible maps with denominator, when the focal points are located on $\overline{LC_{-1}}$. It requires the intersection of a basin boundary with a prefocal curve, followed by the contact of the resulting lobe with a focal point.

4.5 Further remarks

The theory of focal points and prefocal curves is also useful to understand some properties of maps defined in the whole plane $\mathbb{R}^2$, having at least one inverse map with vanishing denominator. Such maps may have the property that, among the points at which the Jacobian vanishes, there exists a curve which is mapped into a single point (see [13]). Another noticeable property of these maps is that a curve, at which the denominator of some inverse vanishes may separate regions of the phase plane characterized by a different number of preimages, even if it is not a critical curve of rank-1 (a critical curve of rank-1 is defined as a set of points having at least two merging rank-1 preimages). At least one inverse is not defined on these non-critical boundary curves, due to the vanishing of some denominator. In a two-dimensional map, the role of such a curve is the analogue of an horizontal asymptote in a one-dimensional map, separating the range into intervals with different numbers of rank-1 preimages [13]. The existence of focal points of an inverse map can also cause the creation of particular attracting sets. Indeed a focal point, generated by the inverse map, may behave like a "*knot*", where infinitely many invariant curves of an attracting set shrink into a set of isolated points, an example is shown in Figure 23, taken from [13]

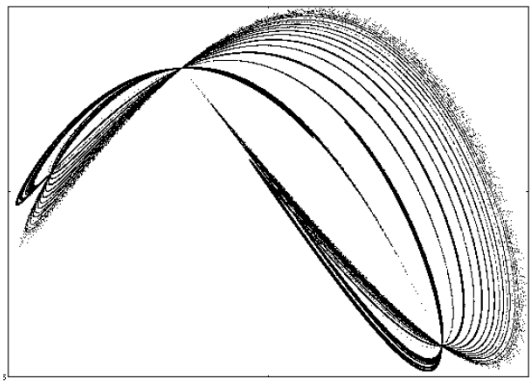

Figure 23.

As already remarked, maps with focal points and prefocal sets naturally arise in discrete dynamical systems of the plane found in several applications, such as economic modeling (see [20] and [18]) or numerical iterative methods (see [6, 25], and [45]). In such dynamic models, peculiar structures of the basins, characterized by the presence of lobes and crescents, have been observed, which can be explained in terms of contacts of two sets of different nature, such as prefocal sets with stable and unstable sets of saddles.

As it was previously mentioned, there are relations between the concepts of focal points and prefocal curve proposed here in the framework of the theory of iteration of two-dimensional real

maps (using the style and terminology of the theory of dynamical systems), and the concepts of exceptional locus and blow-up in the framework of the study of rational maps in the literature on algebraic geometry[6]. It would be very interesting to create a link between these two literature streams.

References

[1] R. H. Abraham and Y. Ueda (eds.) *The Chaos Avant-garde: Memories of the Early Days of Chaos Theory*, Singapore: World Scientific, 2000.

[2] H. N. Agiza, G. I. Bischi and M. Kopel, *Multistability in a dynamic Cournot Game with three oligopolists*, Mathematics and Computers in Simulation **51** (1999), 63–90.

[3] A. Agliari, G.I. Bischi and L. Gardini, *Some methods for the global analysis of dynamic games represented by noninvertible maps*, in T. Puu and I. Sushko (eds.) *Oligopoly Dynamics: Models and Tools*, Springer–Verlag, 2002, pp. 31-83.

[4] J. C. Alexander, J. A. Yorke, Z. You and I. Kan, *Riddled basins*, International Journal of Bifurcation and Chaos **2** (1992), 795–813.

[5] P. Ashwin, J. Buescu and I. Stewart, *From attractor to chaotic saddle: a tale of transverse instability*, Nonlinearity **9** (1996), 703–737.

[6] L. Billings and J. H. Curry, *On noninvertible maps of the plane: eruptions*, Chaos **6** (1996), 108–119.

[7] G. I. Bischi, R. Carini, L. Gardini and P. Tenti, *Sulle Orme del Caos. Comportamenti Complessi in Modelli Matematici Semplici*, Bruno Mondadori Editore, 2004.

[8] G. I. Bischi, H. Dawid and M. Kopel, *Spillover effects and the evolution of firm clusters*, Journal of Economic Behavior and Organization **50** (2003), 47–75.

[9] I. Bischi and L. Gardini, *Basin fractalization due to focal points in a class of triangular maps.* International Journal of Bifurcation & Chaos **7** (1997), 1555-1577.

[10] G. I. Bischi and L. Gardini, *Role of invariant and minimal absorbing areas in chaos synchronization*, Physical Review E **58** (1998), 5710–5719.

[11] G. I. Bischi and L. Gardini, *Global properties of symmetric competition models with riddling and blowout phenomena*, Discrete Dynamics in Nature and Society **5** (2000), 149–160.

[12] G. I. Bischi, L. Gardini and M. Kopel, *Analysis of global bifurcations in a market share attraction model*, Journal of Economic Dynamics and Control **24** (2000), 855–879.

[13] G. I. Bischi, L. Gardini and C. Mira, *Maps with denominator. Part I: some generic properties*, International Journal of Bifurcation & Chaos **9** (1999), 119–153.

[14] G. I. Bischi, L. Gardini and C. Mira, *Unbounded sets of attraction*, International Journal of Bifurcation & Chaos **10** (2000), 1437–1470.

[6] *Editors's note.* See for instance the papers of E. Bedford and K. Kim in these Proceedings, and references therein.

[15] G. I. Bischi, L. Gardini and C. Mira, *Plane maps with denominator. Part II: noninvertible maps with simple focal points*, International Journal of Bifurcation and Chaos **13** (2003), 2253–2277.

[16] G. I. Bischi, L. Gardini and C. Mira, *Plane maps with denominator. Part III: non simple focal points and related bifurcations*, International Journal of Bifurcation and Chaos **15** (2005), 451–496.

[17] G. I. Bischi and M. Kopel, *Equilibrium selection in a nonlinear duopoly game with adaptive expectations*, Journal of Economic Behavior and Organization **46** (2001), 73–100.

[18] G. I. Bischi, M. Kopel, and A. Naimzada, *On a rent-seeking game described by a non-invertible iterated map with denominator*, Nonlinear Analysis, Theory, Methods & Applications **47** (2001), 5309–5324.

[19] G. I. Bischi, L. Mroz and H. Hauser, *Studying basin bifurcations in nonlinear triopoly games by using 3D visualization*, Nonlinear Analysis, Theory, Methods & Applications **47** (2001), 5325–5341.

[20] G. I. Bischi and A. Naimzada, *Global analysis of a nonlinear model with learning*, Economic Notes **26** (1997), 143–174.

[21] G. I. Bischi, L. Stefanini and L. Gardini, *Synchronization, intermittency and critical curves in duopoly games*, Mathematics and Computers in Simulations **44** (1998), 559–585.

[22] G. I. Bischi and F. Tramontana, *Three-dimensional discrete-time Lotka-Volterra models with an application to industrial clusters*, Communications in Nonlinear Science and Numerical Simulations **15** (2010), 3000–3014.

[23] J. Buescu, *Exotic Attractors*, Birkhäuser, Boston, 1997.

[24] R. L. Devaney, *An Introduction to Chaotic Dynamical Systems*, The Benjamin/Cummings Publishing Co., Menlo Park, 1989.

[25] L. Gardini, G. I. Bischi and D. Fournier-Prunaret, *Basin boundaries and focal points in a map coming from Bairstow's method*, Chaos **9** (1999), 367–380.

[26] L. Gardini, G. I. Bischi and C. Mira (2007), in *Maps with vanishing denominators*, in Scholarperdia.org (2007).
`http://www.scholarpedia.org/article/Maps_with_vanishing_denominators`

[27] L. Gardini, F. Tramontana and I. Sushko, *Border collision bifurcations in one-dimensional linear-hyperbolic maps*, Mathematics and Computers in Simulation **81** (2010), 899–914.

[28] J. Guckenheimer and P. Holmes, *Nonlinear Oscillations, Dynamical Systems and Bifurcations of Vector Fields*, Springer-Verlag, 1983.

[29] I. Gumowski and C. Mira, *Dynamique Chaotique. Transition ordre-désordre*, Cepadues Editions, Toulouse, 1980.

[30] I. Gumowski and C. Mira, *Recurrences and Discrete Dynamical Systems*, Springer-Verlag, Berlin, 1980.

[31] C. Grebogi, E. Ott and J. A. Yorke, *Crises, sudden changes in chaotic attractors and chaotic transients,* Physica D **7** (1983), 181–200.

[32] Y. C. Lai and C. Grebogi, *Noise-induced riddling in chaotic systems,* Physical Review Letters **77** (1996), 5047–5050.

[33] Y. Maistrenko, V. L. Maistrenko, A. Popovich and E. Mosekilde, *Role of the absorbing area in chaotic synchronization,* Physical Review Letters **80** (1998), 1638–1641.

[34] Y. Maistrenko, V. L. Maistrenko, A. Popovich and E. Mosekilde, *Transverse instability and riddled basins in a system of two coupled logistic maps,* Physical Review E **57** (1998), 2713–2724.

[35] J. Milnor, *On the concept of attractor,* Commun. Math Phys **59** (1985), 177–195.

[36] C. Mira, *Chaotic Dynamics*, Word Scientific, Singapore, 1987.

[37] C. Mira, *Noninvertinble maps*, in Scholarperdia.org (2007).
`http://www.scholarpedia.org/ article/Noninvertible_maps`

[38] C. Mira, D. Fournier-Prunaret, L. Gardini, H. Kawakami and J. C. Cathala, *Basin bifurcations of two-dimensional noninvertible maps: fractalization of basins,* International Journal of Bifurcation and Chaos **4** (1994), 343–381.

[39] C. Mira and C. Rauzy, *Fractal aggregation of basin islands in two-dimensional quadratic noninvertible maps,* International Journal of Bifurcations and Chaos **5** (1995), 991–1019.

[40] C. Mira, L. Gardini, A. Barugola and J. C. Cathala, *Chaotic dynamics in two-dimensional noninvertible maps.* World Scientific, Singapore, Series on Nonlinear Science, Series A, vol. 20, 1996.

[41] E. Ott and J. C. Sommerer, *Blowout bifurcations: the occurrence of riddled basins and on-off intermittency,* Phys. Lett. A **188** (1994), 39–47.

[42] L. M. Pecora and T. L. Carrol, *Synchronization in chaotic systems,* Physical Review Letters **64** (1990), 821–824.

[43] F. Tramontana and L. Gardini, *Border collision bifurcations in discontinuous one-dimensional linear- hyperbolic maps,* Communications in Nonlinear Science and Numerical Simulation **16** (2011), 1414–1423.

[44] S. C. Venkataramani, B. R. Hunt and E. Ott, *Bubbling transition,* Physical Review E **54** (1996), 1346–1360.

[45] H. C. Yee and P.K. Sweby, *Global asymptotic behavior of iterative implicit schemes,* International Journal of Bifurcation & Chaos **4** (1994), 1579–1611.